AFFDL-TR-71-179

FERROFLUID GYRO

G. Miskolczy and R. Litte
Avco Corporation
Lowell, Massachusetts

AVSD-0093-72-RR

Technical Report AFFDL-TR-71-179
November 1971

Approved for public release; distribution unlimited.

Air Force Flight Dynamics Laboratory
Air Force Systems Command
Wright Patterson Air Force Base, Ohio

55

NOTICE

When Government drawings, specifications, or other data are used for any purpose other than in connection with a definitely related Government procurement operation, the United States Government thereby incurs no responsibility nor any obligation whatsoever; and the fact that the government may have formulated, furnished, or in any way supplied the said drawings, specifications, or other data, is not to be regarded by implication or otherwise as in any manner licensing the holder or any other person or corporation, or conveying any rights or permission to manufacture, use, or sell any patented invention that may in any way be related thereto.

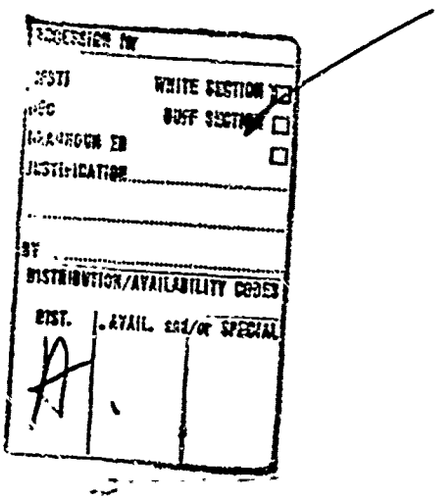

Copies of this report should not be returned unless return is required by security considerations, contractual obligation, or notice on a specific document.

Unclassified
Security Classification

DOCUMENT CONTROL DATA - R & D

(Security classification of title, body of abstract and indexing annotation must be entered when the overall report is classified)

1 ORIGINATING ACTIVITY (Corporate author) Avco Corporation Systems Division Lowell, Massachusetts 01851	2a. REPORT SECURITY CLASSIFICATION Unclassified 2b. GROUP

3 REPORT TITLE

Ferrofluid Gyro

4 DESCRIPTIVE NOTES (Type of report and inclusive dates)

5 AUTHOR(S) (First name, middle initial, last name)

Gabor Miskolczy
Rudolph Litte

6 REPORT DATE November 1971	7a. TOTAL NO OF PAGES 55	7b. NO OF REFS 6
8a. CONTRACT OR GRANT NO F33615-71-C-1060 b PROJECT NO 8222 cTask No. 822203	9a. ORIGINATOR'S REPORT NUMBER(S) 9b. OTHER REPORT NO(S) (Any other numbers that may be assigned this report) AFFDL-TR-71-179	

10 DISTRIBUTION STATEMENT

Approved for public release; distribution unlimited.

11 SUPPLEMENTARY NOTES	12. SPONSORING MILITARY ACTIVITY Air Force Flight Dynamics Lab. AFFDL (FDCL) Wright-Patterson Air Force Base, Ohio 45433

13 ABSTRACT

The concept of using a ferrofluid rotating under the influence of an electromagnetic field as a gyroscope is reported. A ferrofluid is a colloidal suspension of ferromagnetic particles and behaves as a magnetic liquid. It was shown that up to about 100 dyne-cm/cm3 or torque can be transmitted at rates of about 5 KHz using a field strength of about 80 oersted. The direction of the torque was observed to be opposite to the rotation of the surface layer of the fluid, indicating a complex flow pattern in the interior. In a dynamic experiment a signal from a search coil surrounding the rotating ferrofluid was less than 2 microvolts/milliradian, when the system was subjected to angular rates of about 150 degrees/sec.

DD FORM 1473

Unclassified
Security Classification

Unclassified

Security Classification

14 KEY WORDS	LINK A		LINK B		LINK C	
	ROLE	WT	ROLE	WT	ROLE	WT
gyro ferrofluid ferromagnetic liquid magnetic liquid vortex liquid gyro rotating magnetic liquid torque on ferrofluid liquid rotor						

Unclassified

Security Classification

FERROFLUID GYRO

G. Miskolczy and R. Litte

Avco Corporation
Lowell, Massachusetts 01851

AVSD-0093-72-RR

FOREWORD

This report was prepared by the Systems Division of the Avco Corporation, Lowell, Massachusetts under Contract F33615-71-C-1060. The contract was initiated under Project 8222. "Control Data Systems and Instrumentation for Advanced Military Vehicles", and Task 822203, "Exploratory Investigations for Fundamental Support of Flight Control Instrumentation Technology". The work was administered under the direction of the Control Systems Development Branch of the Flight Control Division, Air Force Flight Dynamics Laboratory, Air Force Systems Command, Wright-Patterson Air Force Base, Ohio, by Dr. Tony DeThomas, Project Engineer.

This report covers work performed between 2 November 1970 and 1 November 1971. It was submitted 1 November 1971 and contains no classified information extracted from classified documents.

Mr. G. Miskolczy was Project Director, Mr. R. Litte was in-house Consultant Engineer, and Dr. R. Kaiser was in-house Ferrofluid Consultant. Mr. W.E. Woolhiser designed the electronic circuits.

This technical report has been reviewed and is approved.

C. PURCELL
Acting Chief, Control
Systems Development Branch
Flight Control Division
AF Flight Dynamics Laboratory

ABSTRACT

The concept of using a ferrofluid rotating under the influence of an electromagnetic field as a gyroscope is reported. A ferrofluid is a colloidal suspension of ferromagnetic particles and behaves as a magnetic liquid. It was shown that up to about 100 dyne-cm/cm^3 of torque can be transmitted at rates of about 5 KHz using a field strength of about 80 oersted. The direction of the torque was observed to be opposite to the rotation of the surface layer of the fluid, indicating a complex flow pattern in the interior. In a dynamic experiment a signal from a search coil surrounding the rotating ferrofluid was less than 2 μvolts/milliradian when the system was subjected to angular rates of about 150 degrees/sec.

TABLE OF CONTENTS

Section	Title	Page No.
I	INTRODUCTION	1
	1. Concept of the Ferrofluid Gyro	1
	2. Description of the Ferrofluid Gyro	4
II	TECHNICAL DISUCSSION	4
	1. Introduction	4
	2. Torque Measurements	4
	a. Apparatus	4
	b. Electronic Driver	6
	c. Driver Coil System	14
	d. Measurement of Magnetic Field in Gap	14
	e. Torque Measuring System	14
	f. Results and Discussion	20
	3. Dynamic Measurements	30
	a. Experimental Arrangements	30
	b. Results and Discussion	36
III	CONCLUSIONS	43
	REFERENCES	44

LIST OF ILLUSTRATIONS

Figure	Title	Page No.
1	Concept of the Ferrofluid Gyro	2
2	Block Diagram of Torque Measurement Apparatus	5
3	Electronic Driver	7
3a	Two Phase Signal Generator	7
3b	Low-Pass Filter	8
3c	Buffer Amplifier with Complimentary Outputs	9
3d	Power Amplifier	10
3e	Power Supplies	11
4	Oscillator Characteristics	12
5	Low Pass Filter Characteristics	13
6	Toroidal Cores	15
7	Magnetic Field Calibration	16
8	Detail of Torque Filament Suspension	17
9	Torque vs Driving Field	21
10	Torque vs Frequency	22
11	Torque vs Driving Field	23
12	Torque vs Driving Field	24
13	Torque vs Frequency	25
14	Fluid Magnetization	27
15	Fluid Flow Patterns	29
16	Block Diagram	31
17	Feedback Amplifier Schematic	32
17a	Two-Phase Generator	32

LIST OF ILLUSTRATIONS (Continued)

Figure	Title	Page No.
17b	Low Pass Filter	33
17c	Feedback Amplifier	34
18	Low Pass Filter Attenuation	35
19	Search Coil and Ferrofluid Container	37
20	Photograph of Coil and Driver for the Dynamic Experiments	38
21	Dynamic Experimental Setup	39
22	Detail of Electronics Mounted on Rate Table	40
23	Dynamic Results	42

LIST OF TABLES

Table	Title	Page No.
I	Magnetic Field Calibration	18
II	Properties of Ferrofluid G-59	19
III	Maximum Ferrofluid Torque	28
IV	Dynamic Experiments	41

SECTION I

INTRODUCTION

1. Concept of the Ferrofluid Gyro

Ferrofluids are stabilized colloidal suspensions of superparamagnetic particles. It was recently discovered (Ref. 1) in this laboratory that a volume of ferrofluid can be rotated by the application of a rotating magnetic field. This rotating field results in a torque on the suspended particles by electromagnetic coupling. In turn, the particles are viscously coupled to the bulk liquid resulting in rotation of the total fluid volume. With this technique, torque and rotation may be imparted to the liquid without mechanical coupling limited by the disorienting effects of Brownian motion.

It was conceived that the rotating magnetic particles could be used as the gyroscopic element in a novel ferrofluid gyro in which the change in orientation of the particles could be determined by electromagnetic means.

The goals of this study were to explore the phenomenon of electromagnetically induced torque in a volume of ferromagnetic liquid and to investigate the feasibility of the ferrofluid gyro concept.

2. Description of Ferrofluid Gyro

The ferrofluid gyro consists of a mass of ferrofluid in a container, a system for generating a rotating magnetic field, a means of applying input angular rates and an electromagnetic sensor system to detect gyro output. Each of these components is briefly described below. A conceptual drawing of the ferrofluid particle gyro is shown in Figure 1.

Ferrofluids are stable dispersions consisting of subdomain magnetic particles, typically magnetite, coated with a stabilizing agent in a carrier liquid. Since most inorganic solids are characteristically insoluble in most common liquids and are not easily solvated, the coupling of a magnetic particle to the bulk liquid phase is accomplished by adding a chemical whose structure is such that it can both adsorb on the surface of the particle and be solvated by the carrier liquid. This results in the formation of an essentially bound liquid sheath around each particle. For a hydrocarbon base ferrofluid a typical stabilizer is oleic acid. This molecule contains a polar carboxylic end group that adsorbs on the particle surface and a hydrocarbon moiety that is similar to the dispersing medium in chemical composition. By proper choice of stabilizing agent, magnetic properties can be conferred to a wide range of liquids which include water, hydrocarbons and fluorocarbons.

With very small particles, the solvated sheath is also responsible for the stability of the suspension. In a well-prepared ferrofluid, the particle diameter is small enough and the effective thickness of the sheath is large enough so that when two particles collide, at the minimum distance of separation of the surfaces, the energy associated with the thermal motion is larger than

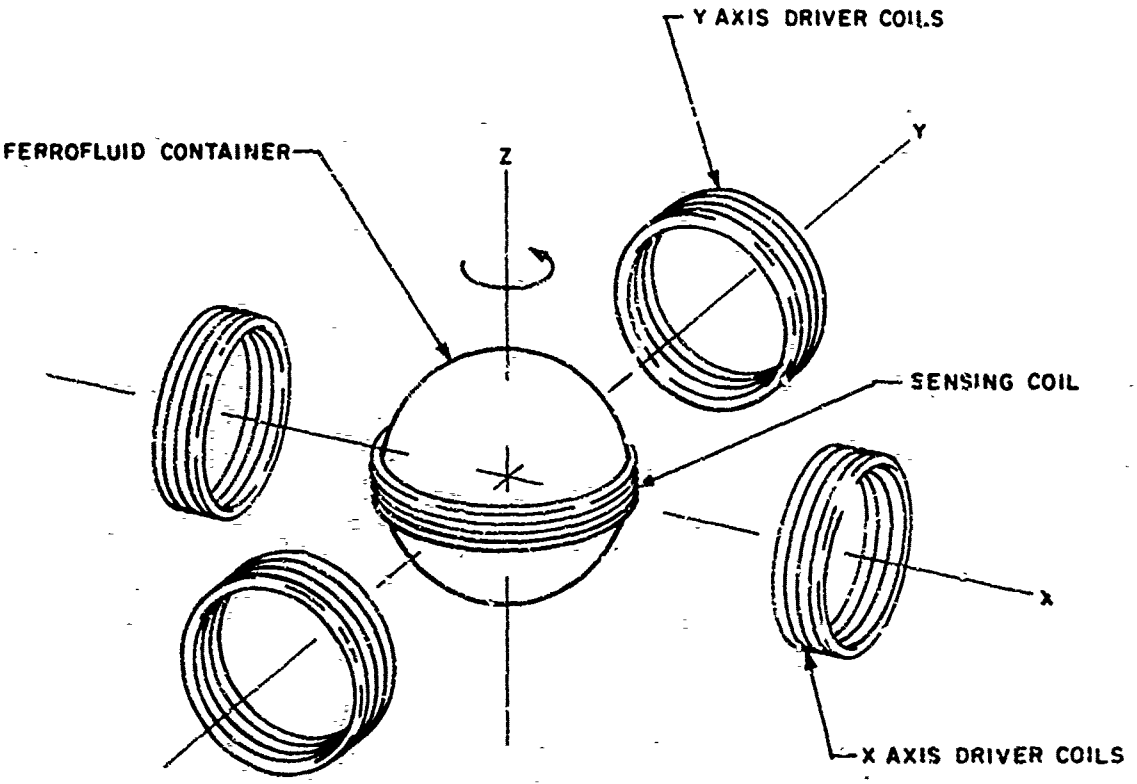

Figure 1 CONCEPT OF THE FERROFLUID GYRO

energy associated with London and magnetic forces of particle interaction. If this were not accomplished, these interparticle forces would rapidly lead to particle agglomeration and gross phase separation. Typically, for a dispersed magnetite ferrofluid, the average particle diameter is usually less than 150 Å and the ratio of the thickness of solvated sheath to the particles diameter is greater than 0.2. The small size results in a very large number of magnetic particles per unit volume, typically 10^{17} particles/cm^3.

A rotating magnetic field is generated by two coils arranged at right angles, driven by a two phase alternating current. A suitable core surrounds the coil system and forms a magnetic flux return path. Since a high frequency is desired to maximize the gyroscopic effect capacitors are used to form a tank circuit with the driver coils to minimize the circuit reactance.

A detector coil, orthogonal to the driving coils, surrounds the ferrofluid container. Thus, the detector coil is sensitive to the precession of the suspended magnetic particles when the ferrofluid is subjected to an angular input rate.

SECTION II

TECHNICAL DISCUSSIONS

1. Introduction

The purpose of this study is to investigate the torque obtainable in a volume of ferrofluid acted upon by a rotating magnetic field. It was shown earlier that significant rotation rates may be induced in such a fluid. A theory to predict fluid rotation and fluid torque was derived in Reference 2. This theory was extended to apply for multi-disperse system in Reference 3. Measurements of the rate of fluid rotation was also reported in Reference 3.

The work reported in Reference 2 concentrated on the measurement of fluid rotation, the present work deals with the measurement of torque and the study of angular rate signals from a volume of rotating ferrofluid instrumented as a gyro. The torque measurements here improve the understanding of the rotating ferrofluid phenomena carried out in the previous studies.

2. Torque Measurements

The purpose of these measurements was to determine the torque developed by a ferrofluid under the influence of a high speed rotating magnetic field. The rotating magnetic field is generated by a system of orthogonal coils driven from a two phase variable frequency power source. The torque on the ferrofluid is measured by a torsional filament suspended at the intersection of the coils.

It was calculated in Reference 3 that fluid torques in the order of 100 dyne-cm/cm^3 could be obtained in a ferrofluid of 100 gauss saturation magnetization. In the present study the torque is to be measured by a torsional filament, as follows. The ferrofluid is in a container at the intersection of the field coils. The electromagnetically induced fluid torque in the ferrofluid rotates the fluid container. This rotation is resisted by torsional rigidity of the suspension filament. The dimensions of the suspension filament are readily selected to yield an angular deflection, which can be easily measured.

In the following subsection the design and construction of the apparatus is described and the results are presented.

a. Apparatus

The block diagram of the torque measuring apparatus is shown in Figure 2. A variable frequency pulse generator feeds a phase shift network. The digital network maintains the two output signals in quadrature. The 0° and 90° outputs of the network are filtered with a variable low pass filter so that the inputs to the power amplifiers are sinusoidal for all driving frequencies. The ferrofluid container is suspended on a torque measuring filament. The torsional filament is calibrated in a separate experiment.

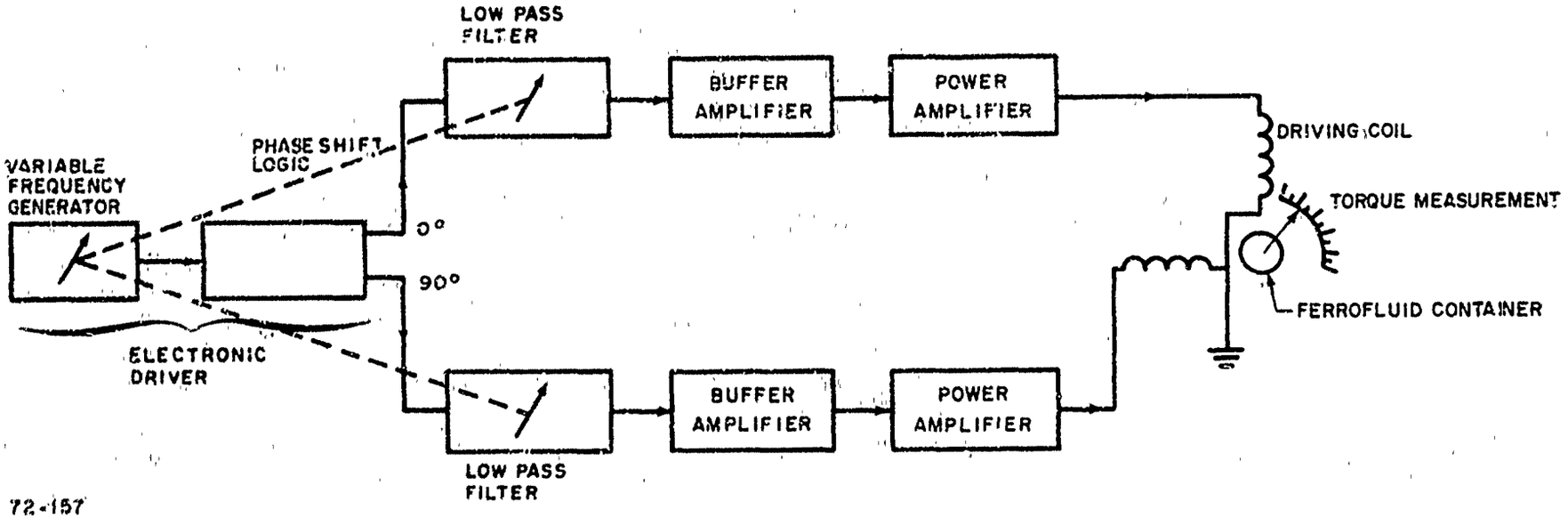

Figure 2 BLOCK DIAGRAM OF TORQUE MEASUREMENT APPARATUS

b. Electronic Driver

The electronic driver shown in Figure 3, consisted of the following parts:

(1) Two Phase Signal Generator (1 each)
(2) Low Pass Filter (2 each)
(3) Buffer Amplifier (2 each)
(4) Power Amplifier (2 each)

These above and a revised power supply are further described below and in Figures 3a - 3e.

Two Phase Signal Generator (Figure 3a)

The signal generator consists of a variable frequency generator and a 90° phase shifting circuit. The driving pulse, is generated by a pair of monostable multivibrators operating at four times the desired frequency. The pulse is fed to a network consisting of flip-flops so that complimentary pulses of one fourth the original frequency are obtained. The multivibrator Z1A determines the pulse repetition rate, variable from 2.5 to 24 sec, while pulse width, determined by Z1B, is maintained at a value sufficient to trigger the rest of the logic, i.e., 200 nsec. The oscillator output goes to the first flip-flop Z2A which is used as a divide-by-two stage. The "0" and "1" outputs of Z2A are connected to the inputs of Z3A and Z3B respectively. The outputs of Z3B are connected to the gates of Z3A to maintain correct phase sequence. The "0" output of Z3A and the "0" output of Z3B are fed to the low pass filters via buffer amplifiers Z4A and Z4B.

The first divide-by-two stage, Z2A, assures a 90° phase difference between the outputs. The additional countdown of two provides a square wave at each output which only contains the fundamental frequency and its odd harmonics, thus reducing the number of poles required in each low pass filter needed to produce a clean sine wave.

Low Pass Filter (Figure 3b)

The low pass active filter has a variable cutoff frequency which is synchronized to the frequency of the driving pulse by a precision, linear 5 gang 50K potentiometer. The first gang is used for the frequency control of the multivibrator, 2 gangs each are used for the filters. The filter cutoff is adjusted to be just above the operating frequency by the proper selection of the 390 PF capacitors. The filter approximately has a 2-pole low pass Butterworth response. Figure 4 shows the frequency output of the phase shift logic with respect to the relative setting of the 5 gang potentiometer control knob. The filter cutoff characteristics corresponding to the minimum driving frequency of 7.3 KHz and the maximum of 35 KHz respectively are shown in Figure 5. It is seen from this figure that the cutoff of the filter is above the operating frequency in each case. It was also observed on an oscilloscope operating in an X-Y mode that the two signals from the filters were sinusoidal and in quadrature for the range of frequencies of 7.3 to 35 KHz.

Buffer Amplifier (Figure 3c)

Each buffer amplifier provides a high impedance load to the filters and produces a balanced "push-pull" output. The low pass filter outputs are coupled to the amplifier inputs through a 2 gang attenuator.

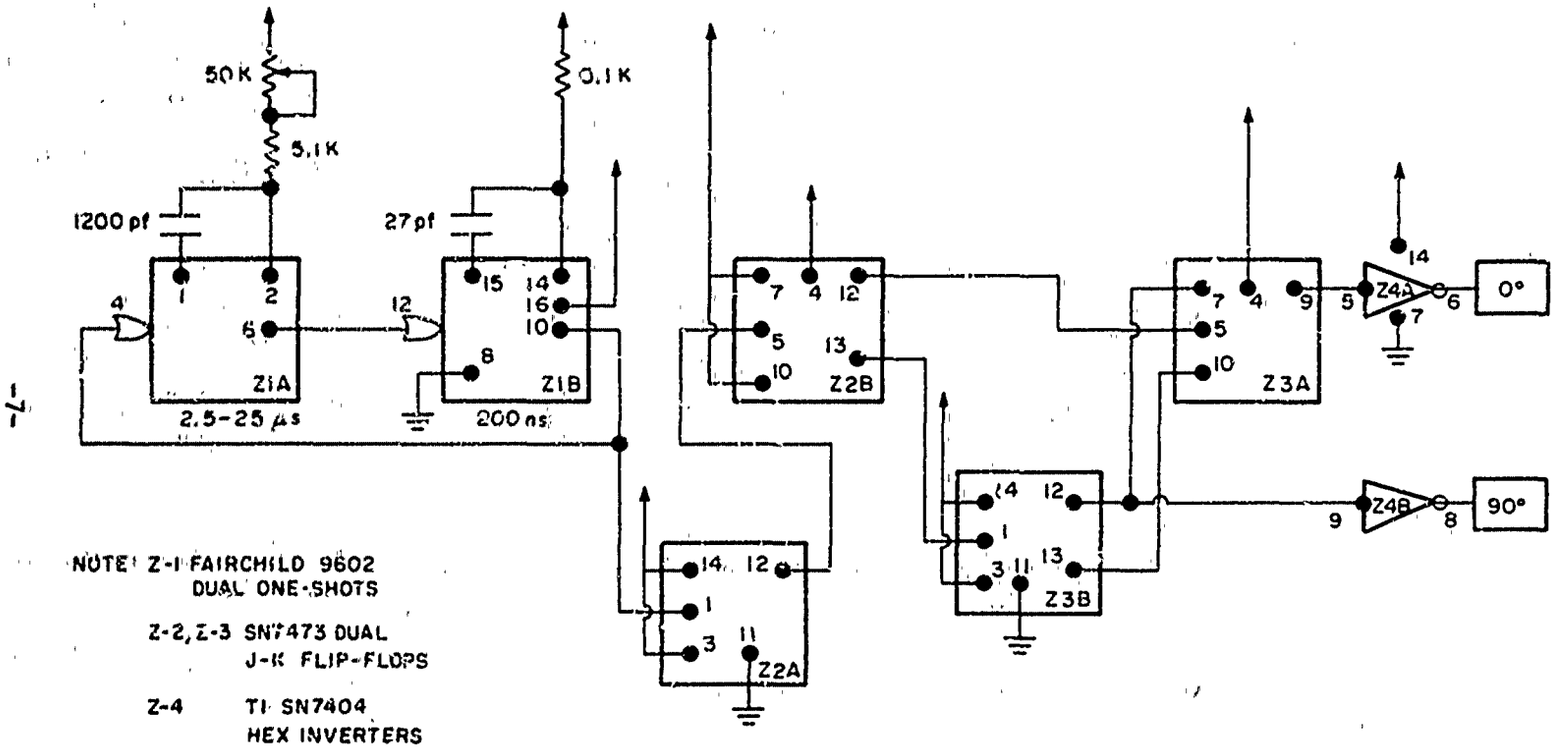

Figure 3 ELECTRONIC DRIVER

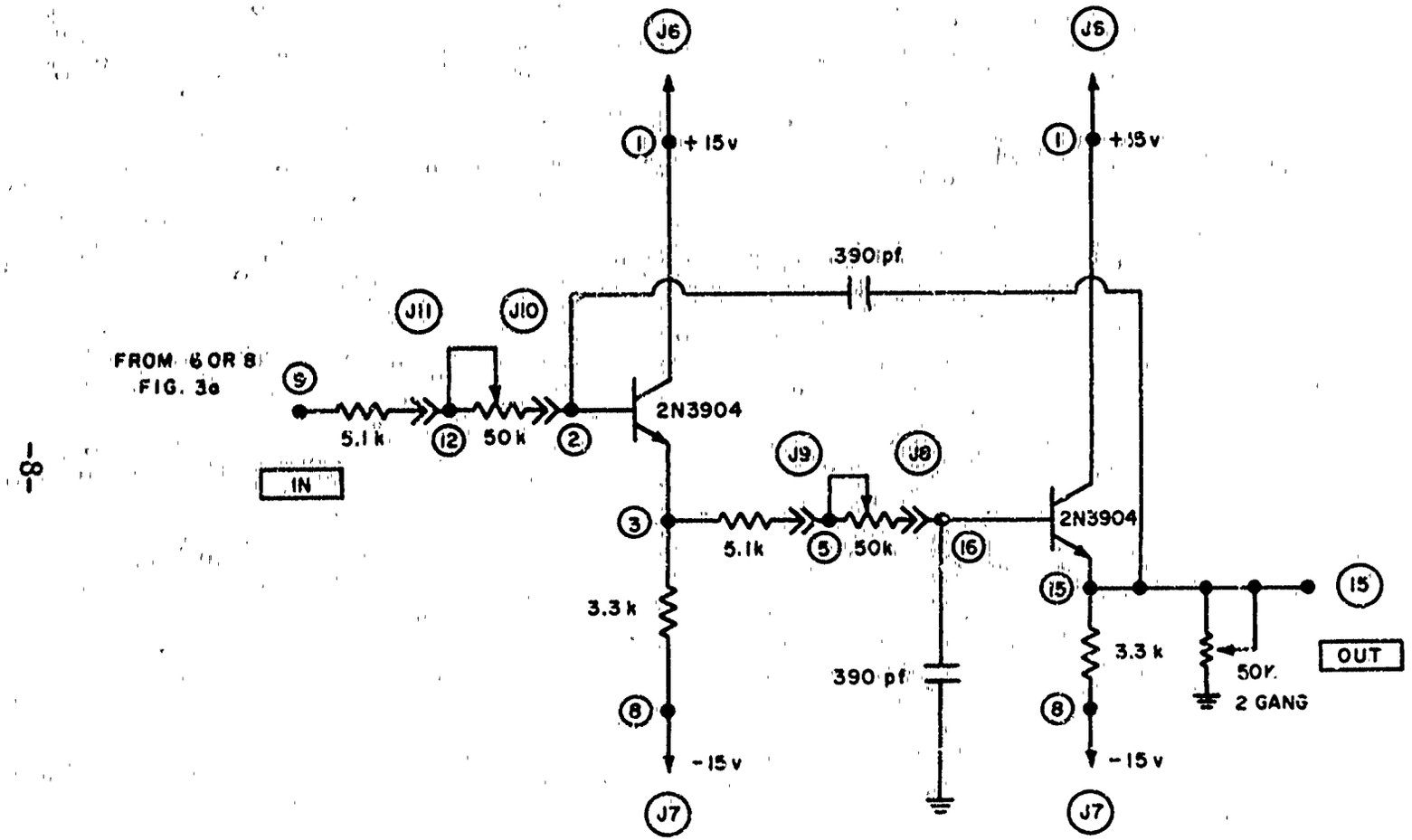

72-153

Figure 3b LOW PASS FILTER

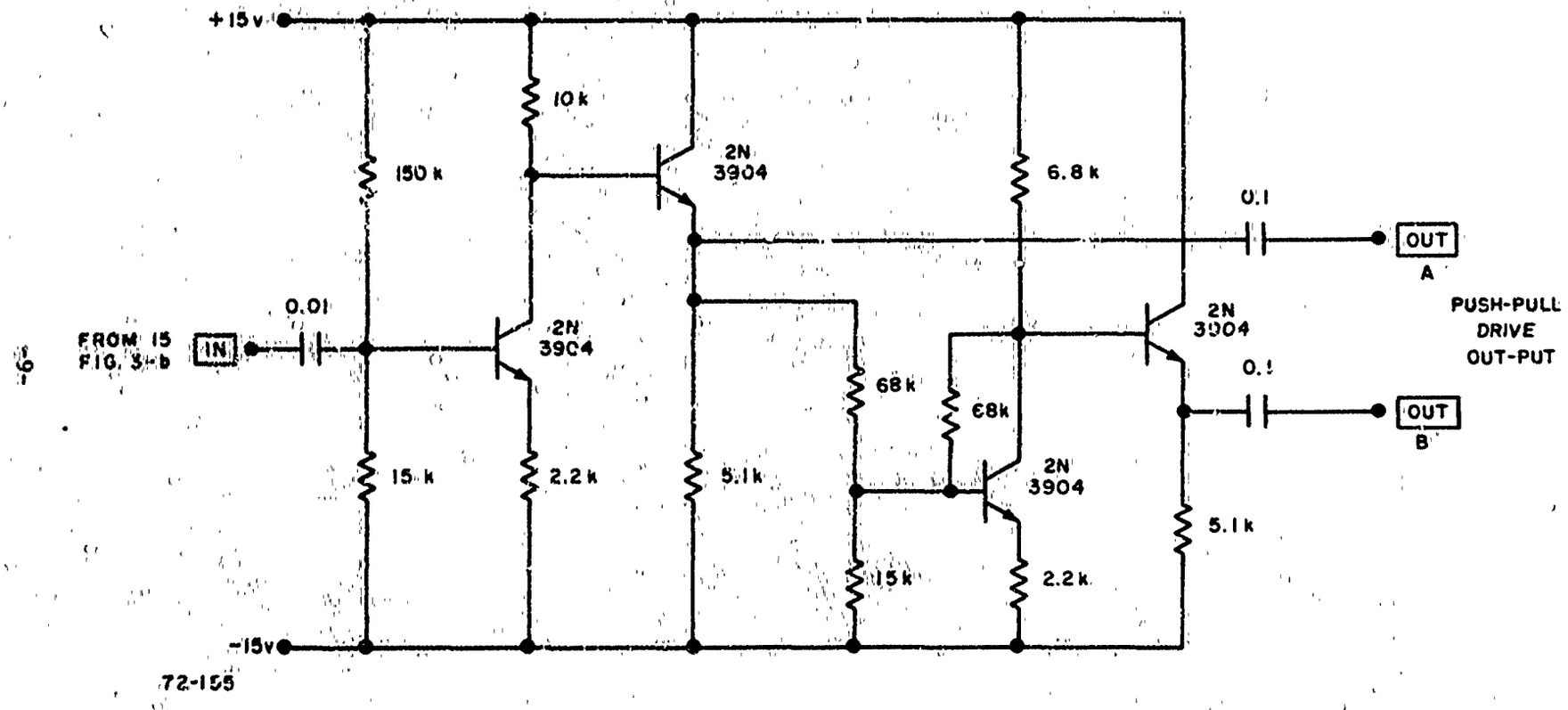

Figure 3c BUFFER AMPLIFIER WITH COMPLIMENTARY OUTPUTS

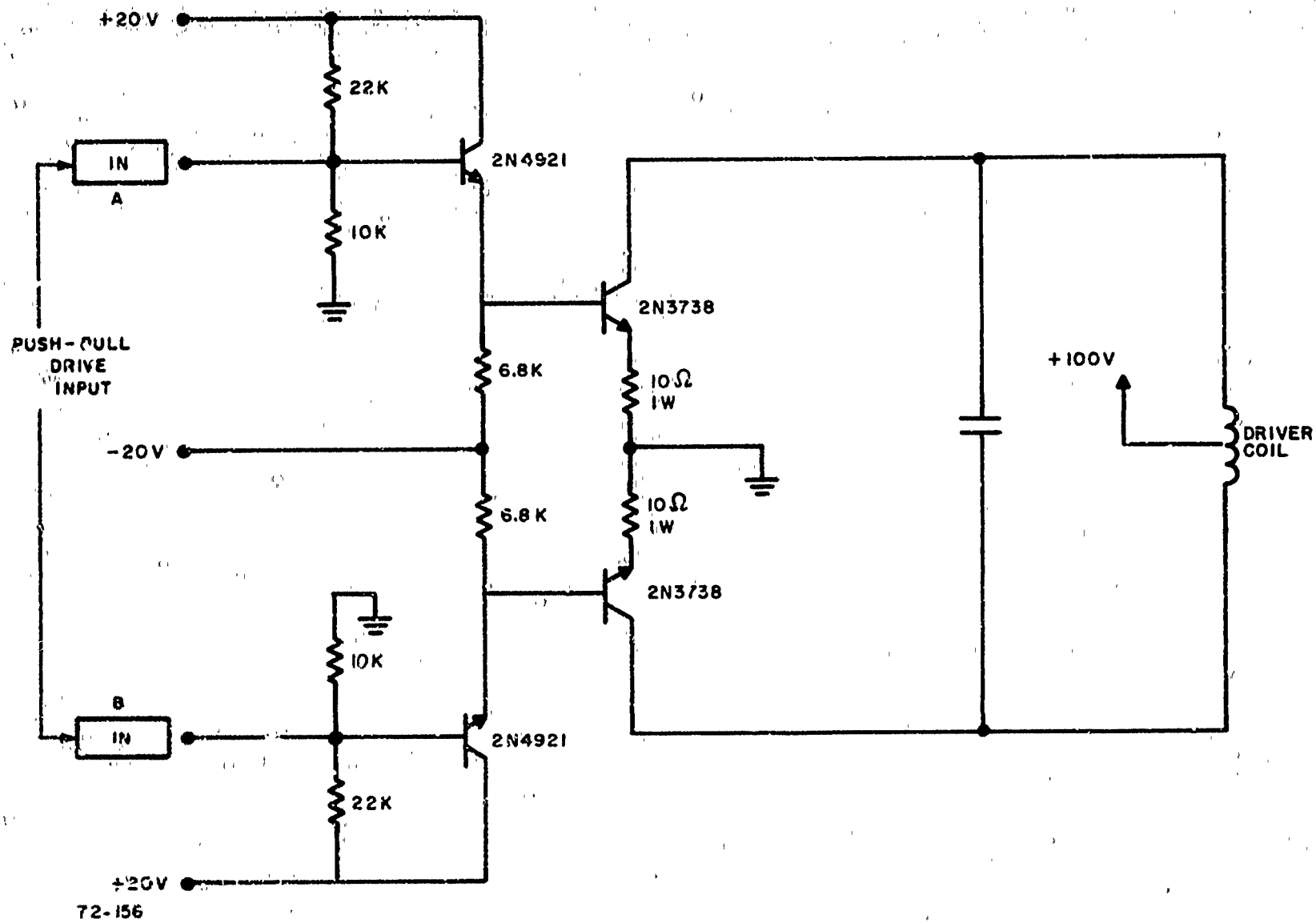

Figure 3d POWER AMPLIFIER

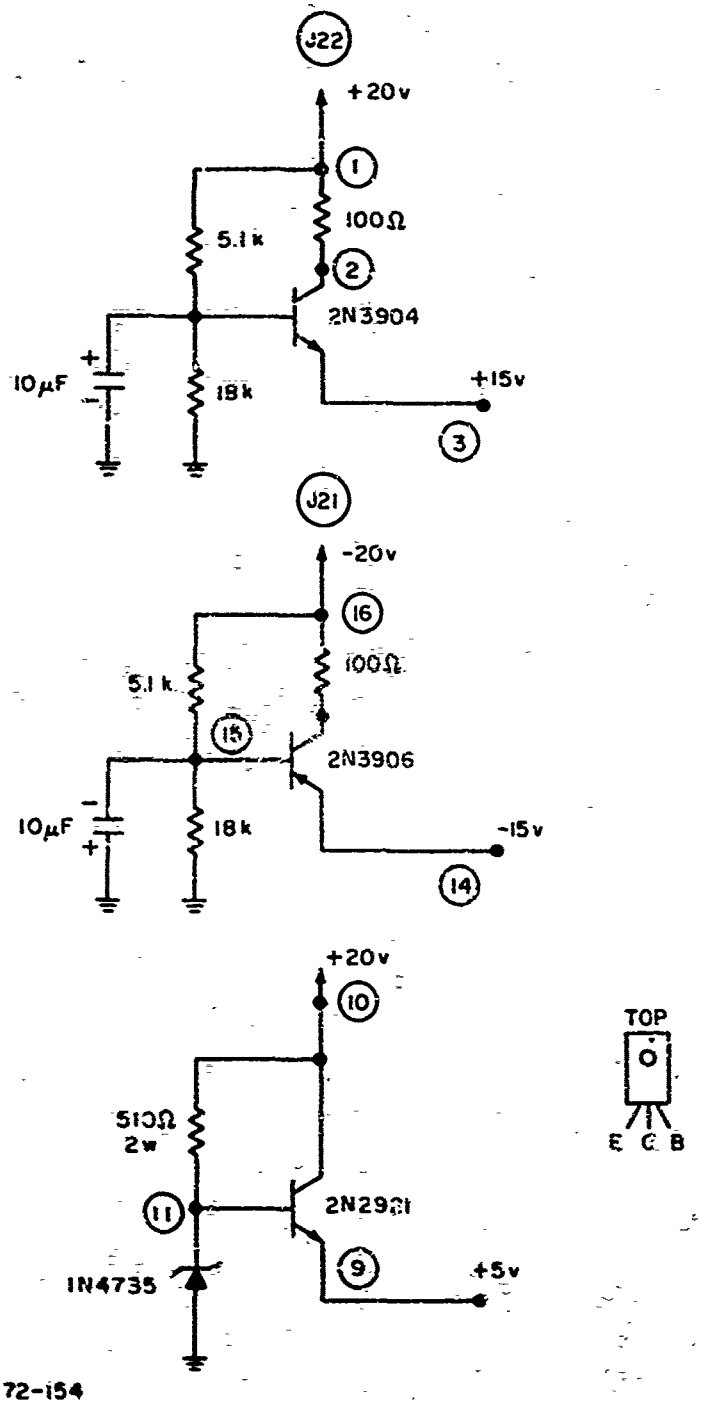

Figure 3e POWER SUPPLIES

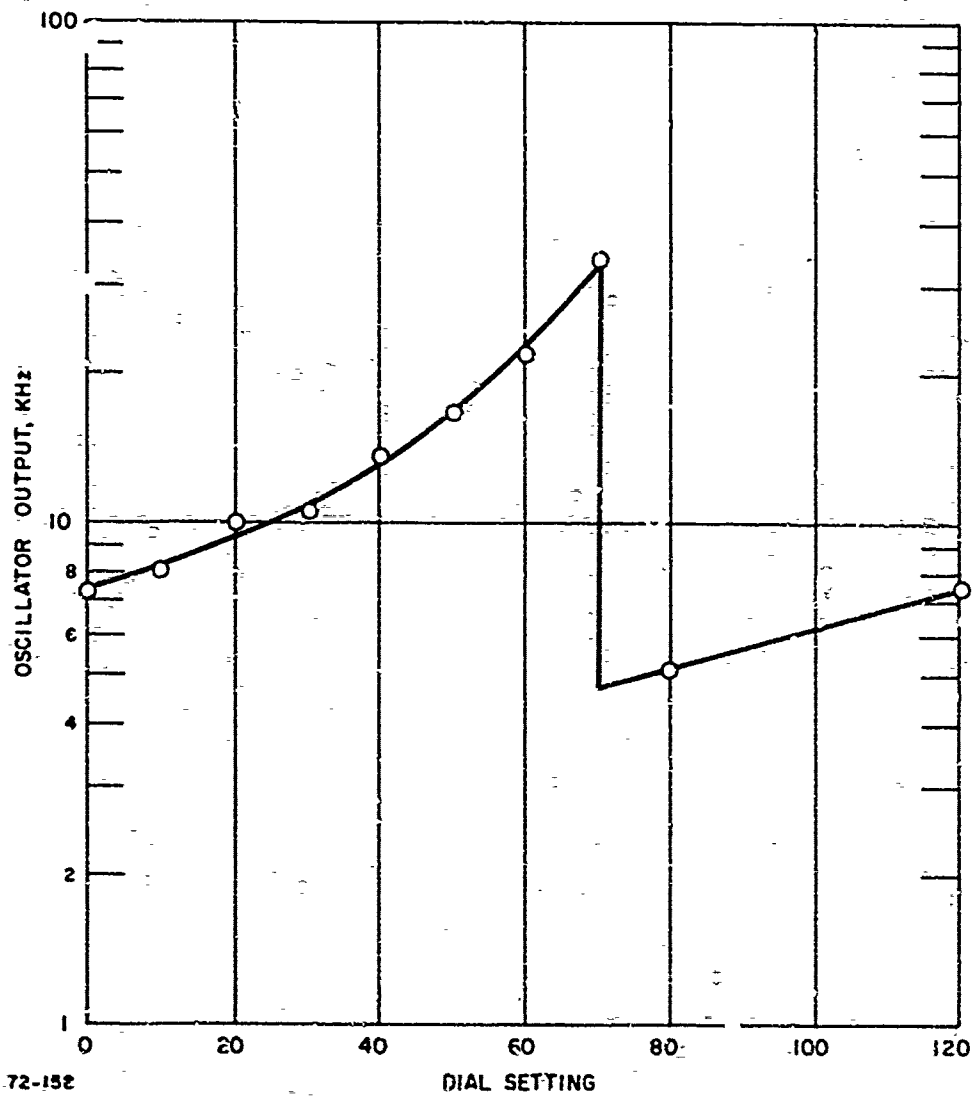

Figure 4 OSCILLATOR CHARACTERISTICS

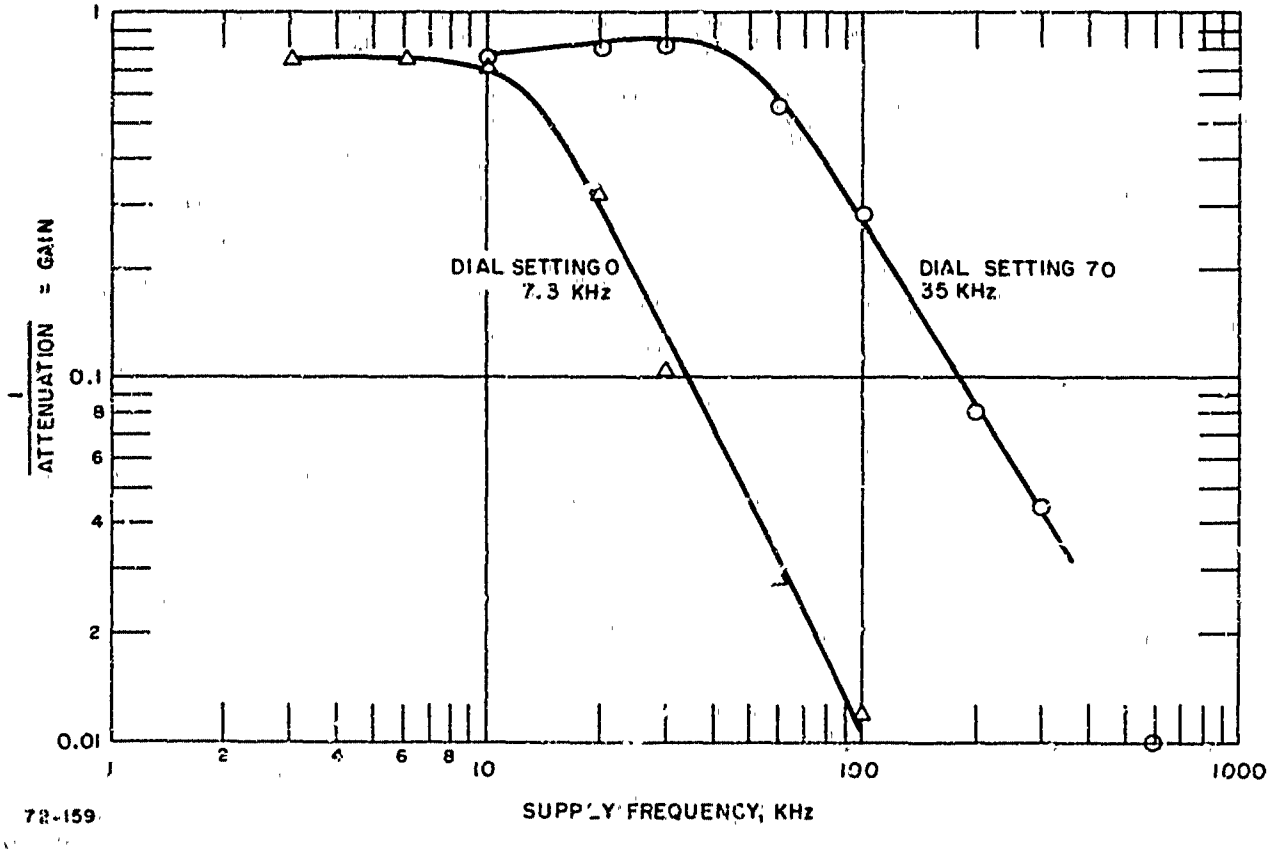

Figure 5 LOW PASS FILTER CHARACTERISTICS

Power Amplifier (Figures 3d and 3e)

The power amplifier provides a high current source to drive the center tapped driver coils. As shown in Figure 3d, capacitors were placed across the driver coils to greatly increase circulating currents. The output was allowed to swing about ±30 volts to supply the voltage necessary to overcome the inductive reactance of the driver coils at the operating frequency.

c. Driver Coil System

The driver coils consist of 24 turns of #13 heavy Formvar copper wire wound on a powdered iron (Carbonyl HP) core, as shown in Figure 6. The toroid ID is 2.000 inch, the OD is 3.150 inch and the width is 0.450 inches. A gap of 0.562 inch wide was cut in each toroid and the toroids were arranged orthogonally as shown in Figure 6 resulting in a working gap 0.562 in by 0.552 in and 0.450 in high. This figure also shows the principal dimensions of the cores.

d. Measurement of Magnetic Field in Gap

Measurements of the magnetic field obtained in the working gap of the coils were obtained with DC and 60 Hz excitation in separate experiments. Equipment limitations precluded measurements at higher frequencies. A single gapped toroid wound with 24 turns of #13 wire was connected to a power supply. A Hall effect gaussmeter probe (C.S. Walker Model FM1) was placed at the midpoint of the gap. The resulting current vs field curves are shown in Figure 7. The coil excitation was varied from 0 to 20 amps dc and 0 to 14 amps rms, 60 Hz. The calibration constant to be used for the torque experiments is obtained by the vectorial addition of the two orthogonal fields. The calibration constant for the dynamic experiment, where 48 turns of #13 wire were used in each core is obtained from the measured values by the usual relation for the gap field, Hg, field of an iron solenoid

$$H_g = \frac{4\pi NI}{10} \frac{1}{\frac{l_g}{\mu_g} + \frac{l_c}{\mu_c}} \qquad 2\text{-}1$$

where N is the number of turns, I is the coil current l_g and l_c are the effective gap and core length, respectively and μ_g and μ_c are the permeabilities of the gap and the core respectively. With air in the gap, $\mu_g = 1$. With coil current, core geometry and material constant the gap field is proportional to the number of turns. Thus, with the same coil current the gap field the dynamic experiments is twice that for the torque experiments, since in latter experiments twice the number of turns are used. The calibration constants shown in Table I are used in the reduction of the experimental data.

e. Torque Measuring System

The ferrofluid container is suspended on a filamentary suspension system as shown in Figure 8. As the ferrofluid in the container rotates under the influence of the externally applied rotating magnetic field the viscous drag on the container causes torsion of the suspension filament.

A light weight non-metallic pointer attached to the ferrofluid container rotating along a scale calibrated in degrees is used to measure the torque readout. The filament used for the suspension is a nylon ribbon of rectangular cross section of 0.0035 inches by 0.018 inches. The torque per degree T/θ for a unit length of ribbon is given by Timoshenko (Reference 5).

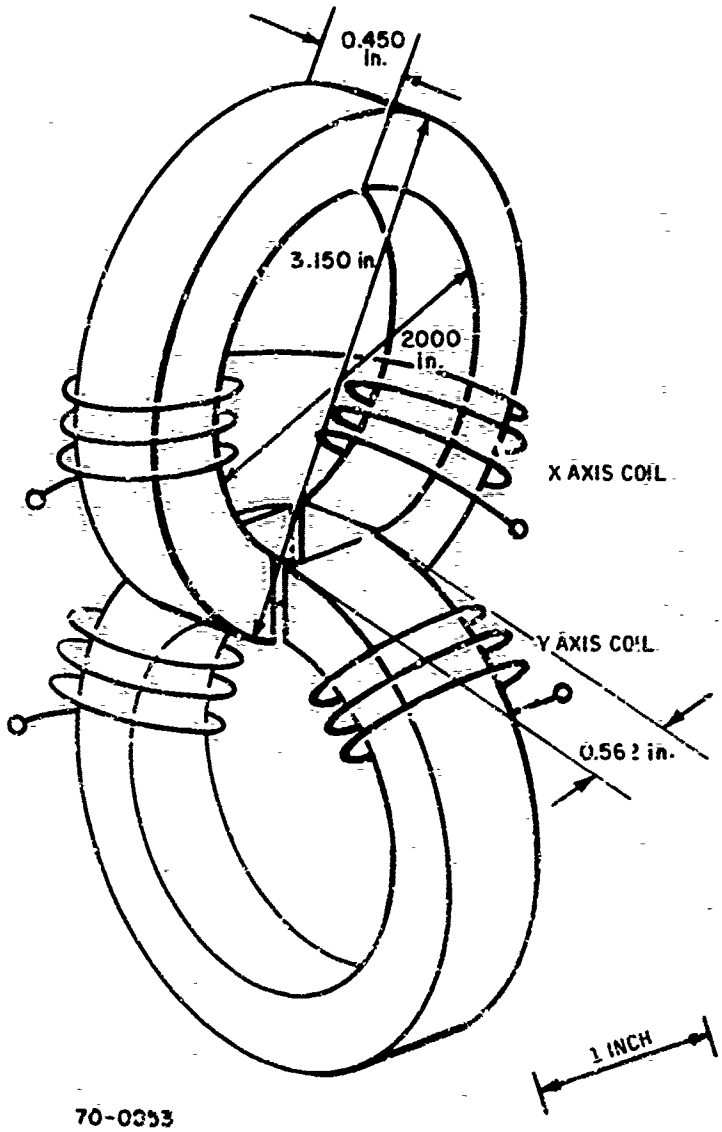

Figure 6 TOROIDAL CORES

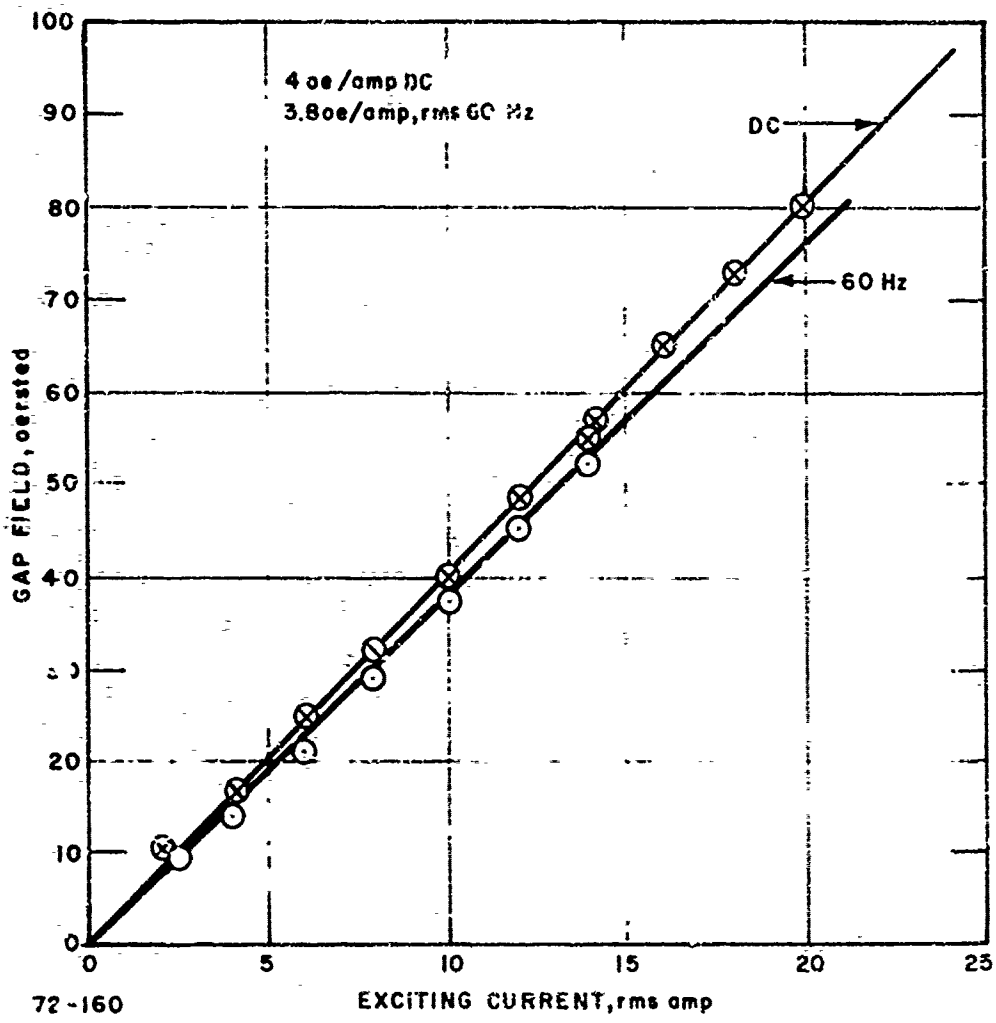

Figure 7 MAGNETIC FIELD CALIBRATION

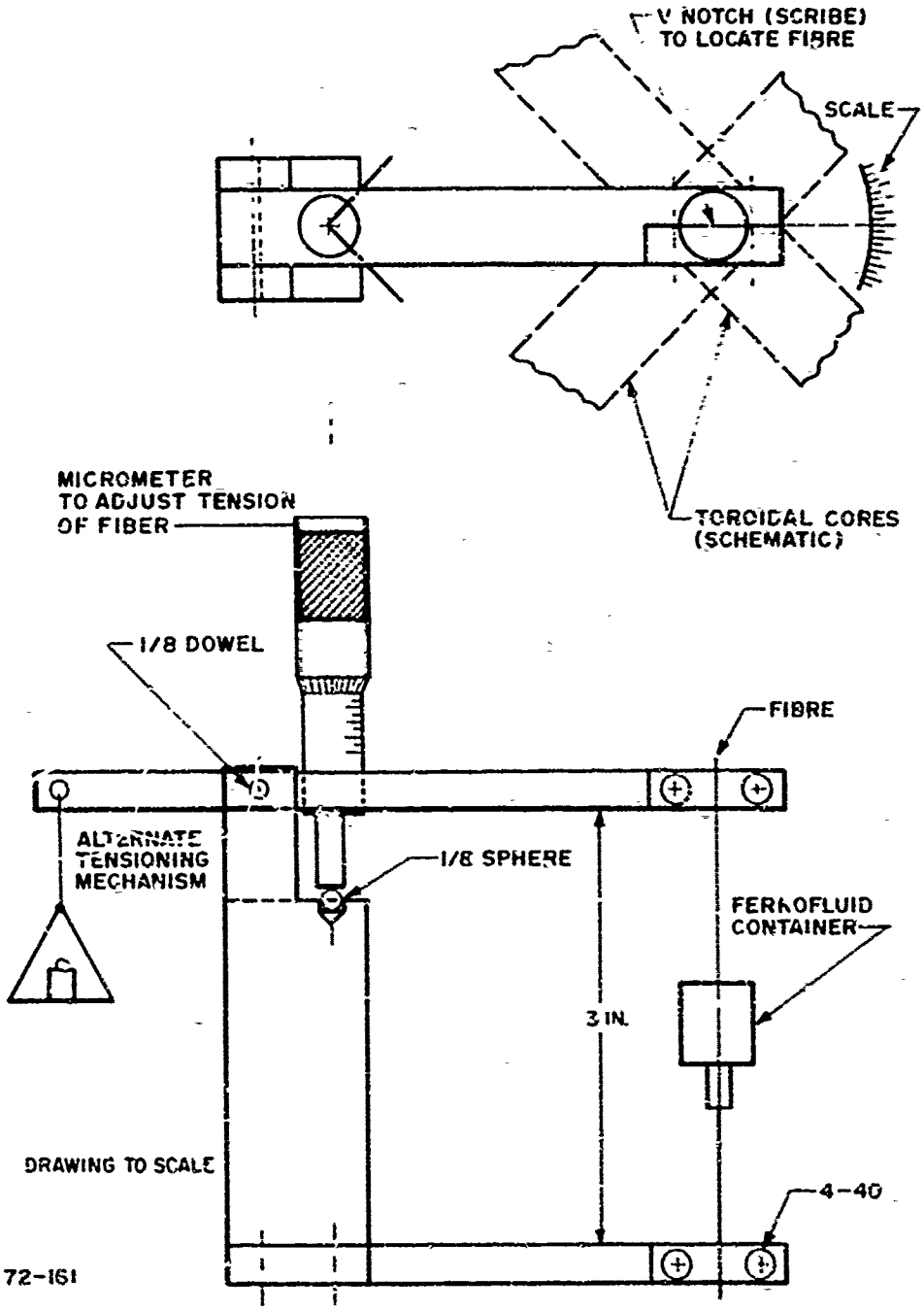

Figure 8 DETAIL OF TORQUE FILAMENT SUSPENSION

TABLE I

MAGNETIC FIELD CALIBRATION

	Calibration			
	DC	60 Hz	Torque Exp.	Dynamic Exp.
Wire Size No.	13	13	13	13
No. of Turns	24	24	24	48
Gap In.	0.562	0.562	0.562	0.562
Constant for 1 Channel Oersted/amp rms	4.0	3.8	3.8	7.6
Constant for 2 Channels 2 Phase Operation Oersted/amp rms	-	-	5.35	10.7

$$\frac{T}{\theta} = bc^3 \beta G \qquad 2\text{-}2$$

where b is the longer and c the shorter side of the rectangular cross section and β is a numerical factor in cm^{-4} (also tabulated in Reference 5) that depends on b/c. G is the modulus of torsional rigidity (dynes-cm/degree). For the present case, b/c = 5.15, giving $\beta(b/c) = 0.290\ cm^{-4}$. Since the modulus of rigidity of the suspension ribbon is not known, an approximate handbook value shall be used to estimate the expected stiffness. The torsional modulus for nylon is given (Reference 6) as 3.0 to 3.6 x 10^9 dyne/cm^2 depending on the history of the material. Using a value of 3.6 x 10^9 dyne/cm^2 and a gage length of 3.5 cm, T/G = 0.812 dyne-cm/deg.

Owing to the difficulty of finding the precise value of torsional rigidity, the actual stiffness of the suspension is measured experimentally, with a separate apparatus. In this apparatus the filament is tensioned by a weight while the ends are prevented from rotating. A torque arm is cemented in the middle, accepts a small rider of known weight at a known radius, the resulting rotation of the filament is observed. The effective lever arm and the torsional stiffness of the ribbon is then calculated. For this experiment the weight of the rider is 30.9 milligrams, the deflection 20 degrees, and the length of the lever arm 1 cm. The effective lever arm is then 1 x cos 20° = 0.94 for a filament gage length of 4.12 cm. The observed deflection did not change when the tension was varied from 10 to 20 grams. The observed stiffness was then 1.45 dyne-cm/deg. Adjusting this value to a gage length of 3.5 cm for the gyro experiment the stiffness is 1.24 dyne-cm/deg.

TABLE II

PROPERTIES OF FERROFLUID G159

FERROFLUID PROPERTIES
FERROHYDRODYNAMICS LABORATORY

FLUID NO.	G159

INVESTIGATOR	PM	
DATE	7 July 69	
MAGNETIZATION, gauss at 10 kilo-oersted	139	
MAGNETIZATION, gauss at 0.12 kilo-oersted	79	
DENSITY, gr/ml	1.13	
VISCOSITY		
TEMP, °C	SHEAR RATE sec-1	VISCOSITY centipoise
30	230 to 11	3.10 ± .15
REMARKS: Water Base		

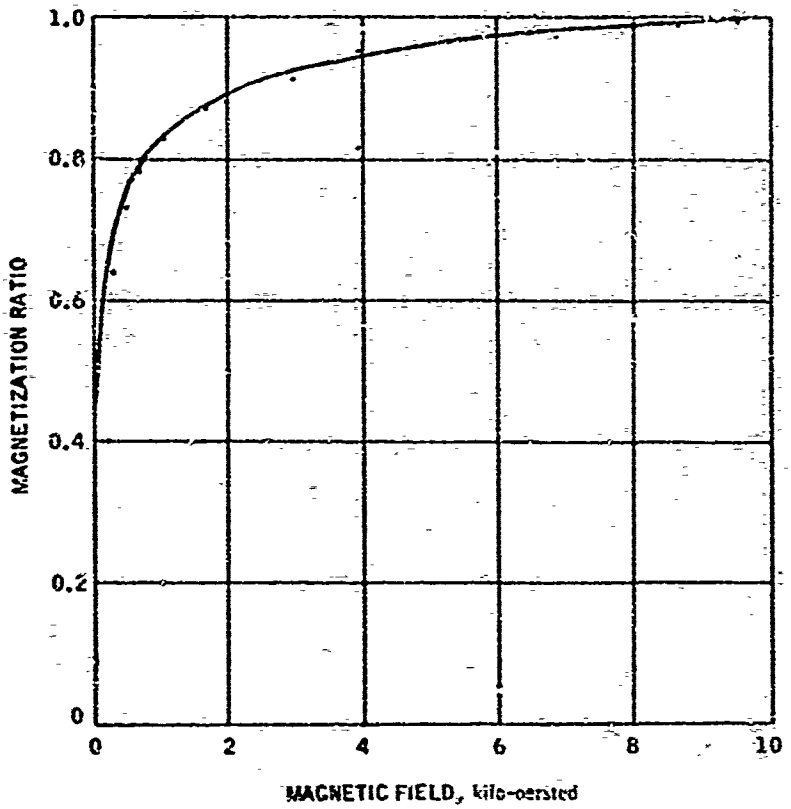

This value is in reasonable agreement with the calculated value of 0.812 dyne-cm/deg when it is recognized that an average handbook value of the torsional rigidity was used. The experimentally observed stiffness value is used in the reduction of the gyro data.

f. Results and Discussion

For the systematic collection of data of observed gyro torque versus driving field magnitude and frequency, the ferrofluid container was filled with 2 ml of G159 ferrofluid. The principal properties of this ferrofluid are shown in Table II. The quadrature of the currents was monitored on an oscilloscope operating in an x-y mode. The driving field magnitude and frequency were also measured with an oscilloscope operating in an x-t and y-t mode.

For the first set of torque measurements the filament was tensioned to 20 gr by a micrometer screw, as shown in Figure 8. For these experiments the driving frequency was varied from 6.2 to 50 KHz, the driving field was varied from 2.5 to 70 oersteds, as shown in Figure 9. It is seen from the figure that the torque varies approximately linearly with field magnitude, and that the torque increases with decreasing frequency. The data of Figure 9 have been replotted versus frequency for 10, 20, and 40 oersted driving field, as shown in Figure 10.

In a separate experiment talcum powder was placed on the free surface of the ferrofluid to assist in visualizing the fluid motion. It was observed that the fluid surface rotated in a direction opposite to that of the container. This phenomenon was also observed by others (Reference 3).

In a second set of torque experiment the micrometer tensioning mechanism was replaced by a 23 gr dead weight, constant tension mechanism. In addition the driving circuit parameter were altered to lower the minimum possible frequency of the driver. This resulted in a change of the output waveform and a consequent difficulty of turning the coil tank circuit capacitors. The results for this set of experiments are shown in Figure 11 and 12. These results are similar, but not identical to those shown in Figure 9.

The scatter in the data believed due to the variations are changes in waveform at different power levels. In these experiments it was not possible to independently control waveform and power level. Existence of a waveform effect is also reflected by the scatter of the torque versus frequency data presented in Figure 13. Based on existing data, it is however difficult to postulate the nature of this previously unknown effect.

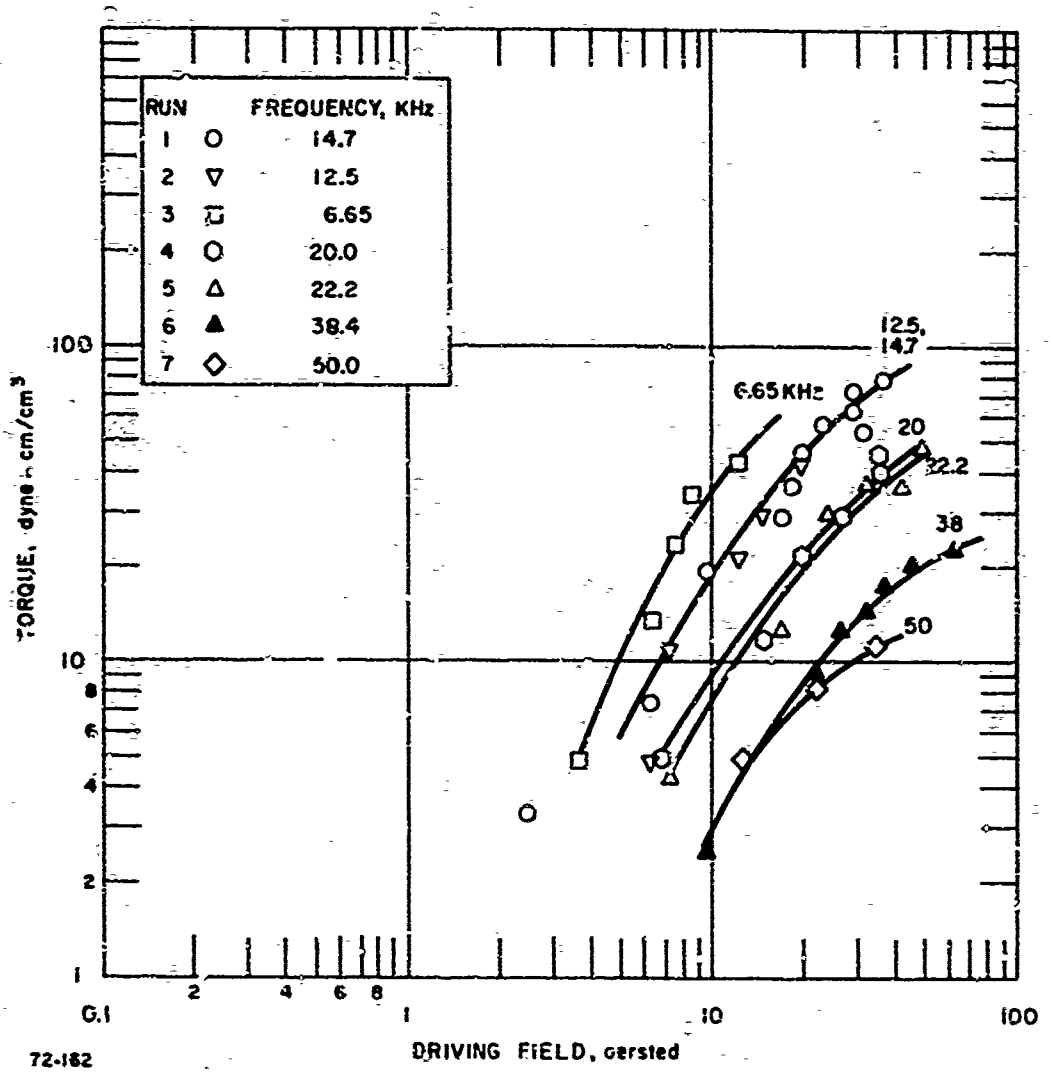

Figure 9 TORQUE VERSUS DRIVING FIELD

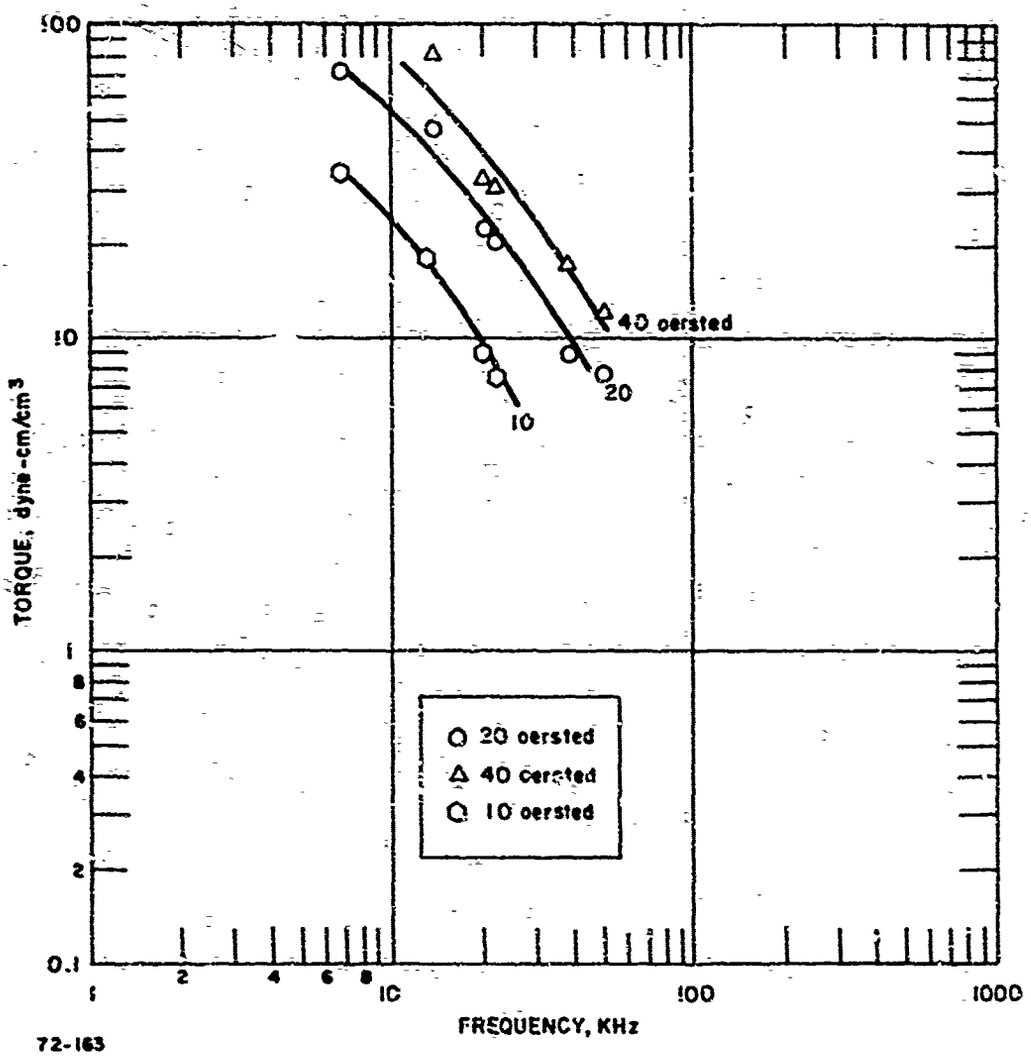

Figure 10 TORQUE VERSUS FREQUENCY

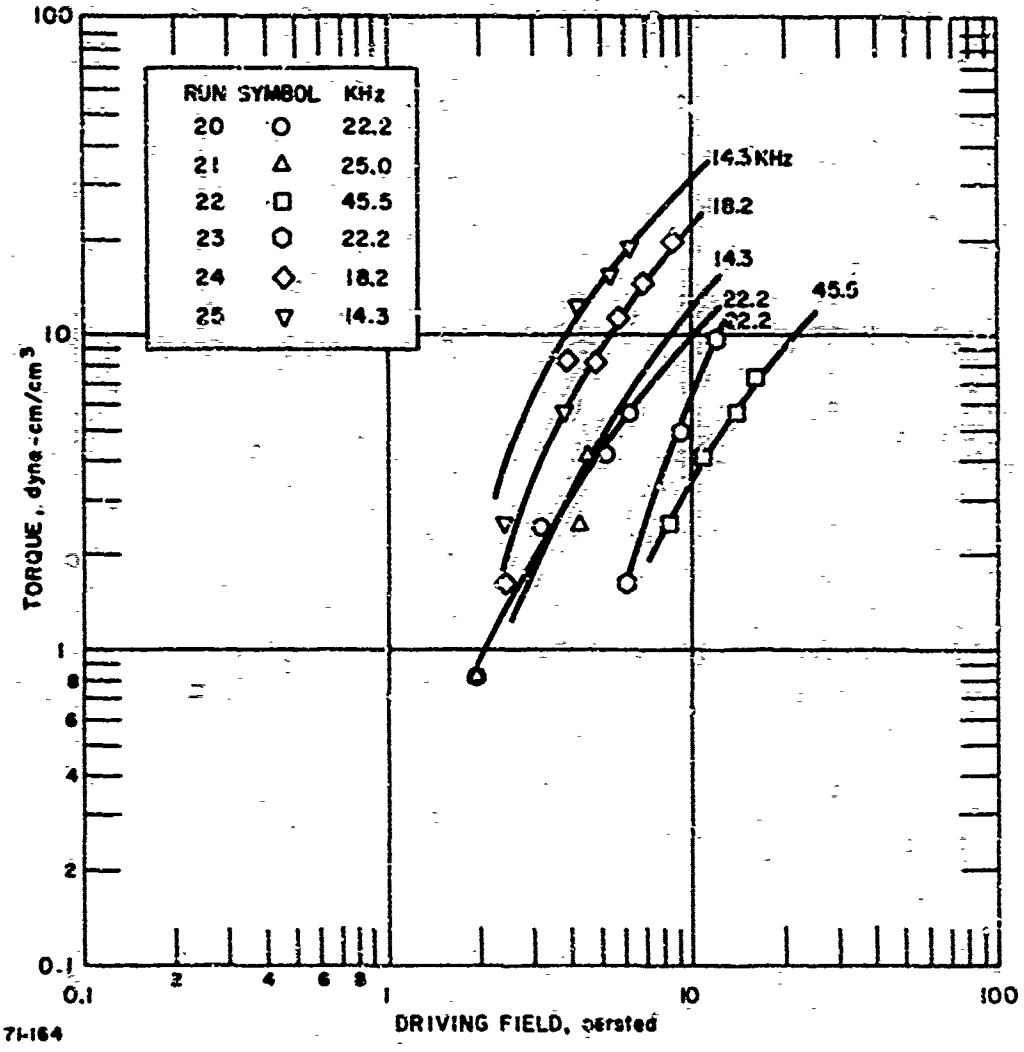

Figure 11 TORQUE VERSUS DRIVING FIELD

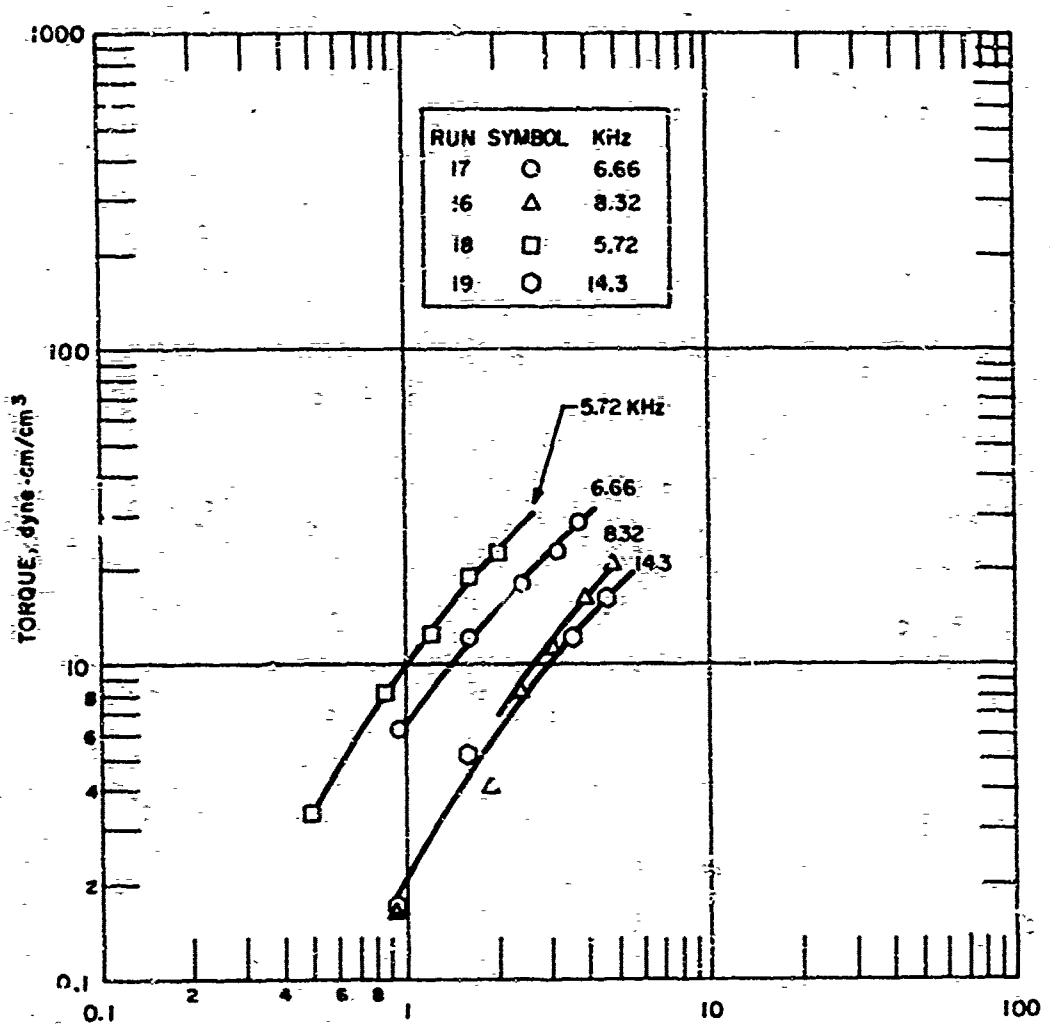

Figure 12 TORQUE VERSUS DRIVING FIELD

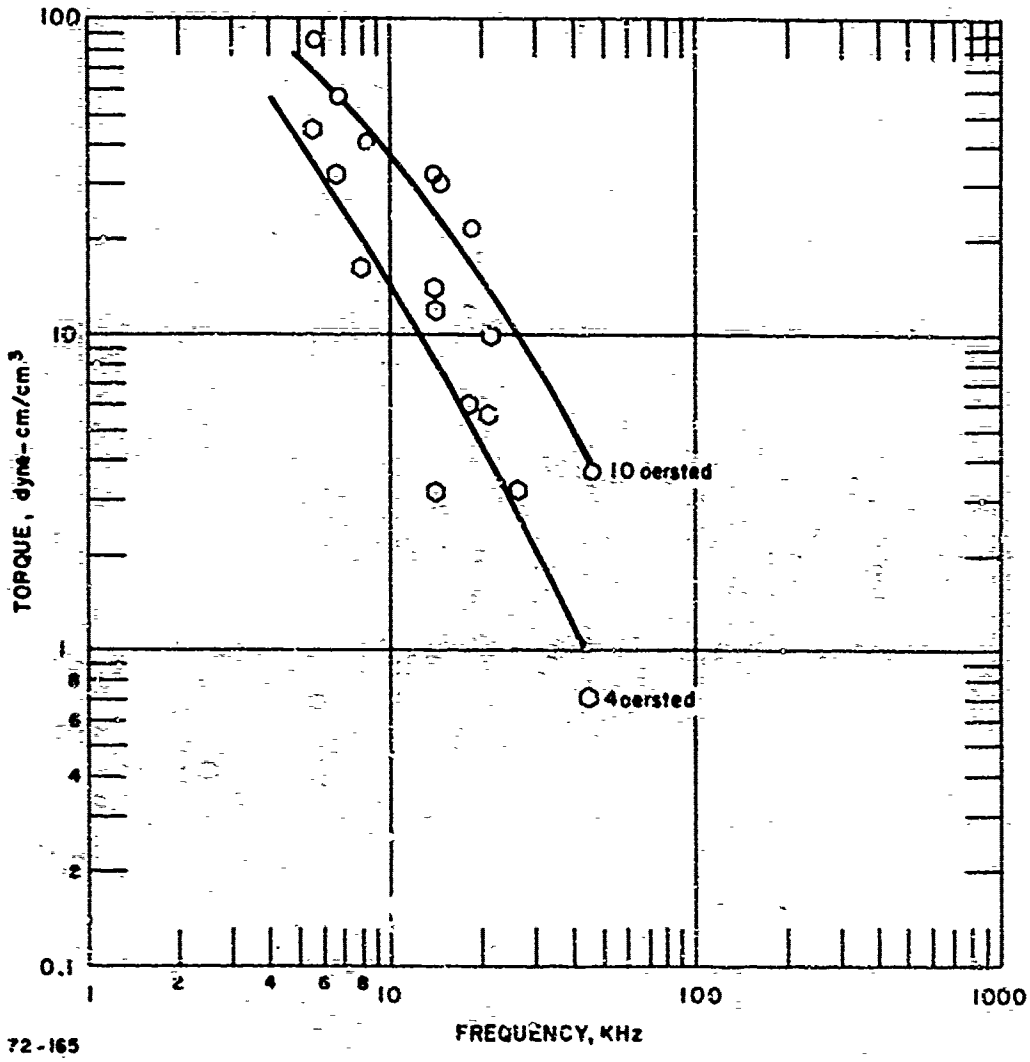

Figure 13 TORQUE VERSUS FREQUENCY

These results may be compared to the predicted torques as follows. It was shown earlier (Reference 2) that the maximum fluid torque, L_{max}, is

$$L_{max} = \frac{1}{4} \chi H_o^2 \qquad 2\text{-}3$$

where χ is the fluid susceptibility and H_o the magnitude of the magnetic field. Equation 2-3 is used to calculate the maximum torque obtainable from theory. The susceptibility for the fluid, ($\chi = M/H$ by definition), is obtained from the shape of the experimentally obtained M vs H curve. Such a curve for Fluid G159A is shown in Figure 14 taken with an automatic curve tracer. In the region near the origin the difficulty of computing the local $\chi = M/H$ is increased by the presence of irregularities in the curve, especially in the region H ≈ 10 oe. From Reference 3 it is noted that for small fields the susceptibility is proportional to the magnetization. Thus the χ at H = 10 oe may be obtained from χ at H_o = 50 oe by interpolation. Thus at H = 10 oe, χ = 2. Following the method of Reference 3 χ may also be calculated from the known ferrofluid particle distribution using Equation 14 of Reference 3:

$$\chi = \frac{\epsilon_m M_s^2}{72\,kT} \frac{\sum n_i (d_i - 2x)^6}{\sum n_i (d_i - 2x)^3}$$

ϵ_m = volume fraction solids

n_i = number of particles of diameter d_i

x = thickness inert outer layer on particles

K = Boltzmann's constant = 1.37×10^{-16} erg/°K

T = Absolute temperature

M_s = Saturation magnetization of solids in suspension.

For ferrofluid G159 the susceptibility was calculated χ = 1.02 at H = 10. For the present experiment, a fluid from the same family with a higher magnetization was used, (M at 10,000 oe = 225 gauss for G159A vs 137 gauss for G159).

The results of these calculations are shown in Table III.

It is also seen in Reference 3 that the frequency for maximum torque w_{max} transmission is given by

$$w_{max} = \frac{kT}{4\pi \eta a^3} \qquad 2\text{-}4$$

where η is the fluid viscosity, and a is the effective solvated radius. In Reference 2 the measured ferrofluid particle distribution was taken and the corresponding bound stabilizing layer yielded an average particle radius of 1.29×10^{-16} cm. From equation 2-4 a frequency of 24.3 KHz is calculated. The experimental observation shows however, that the maximum torque occurs at a

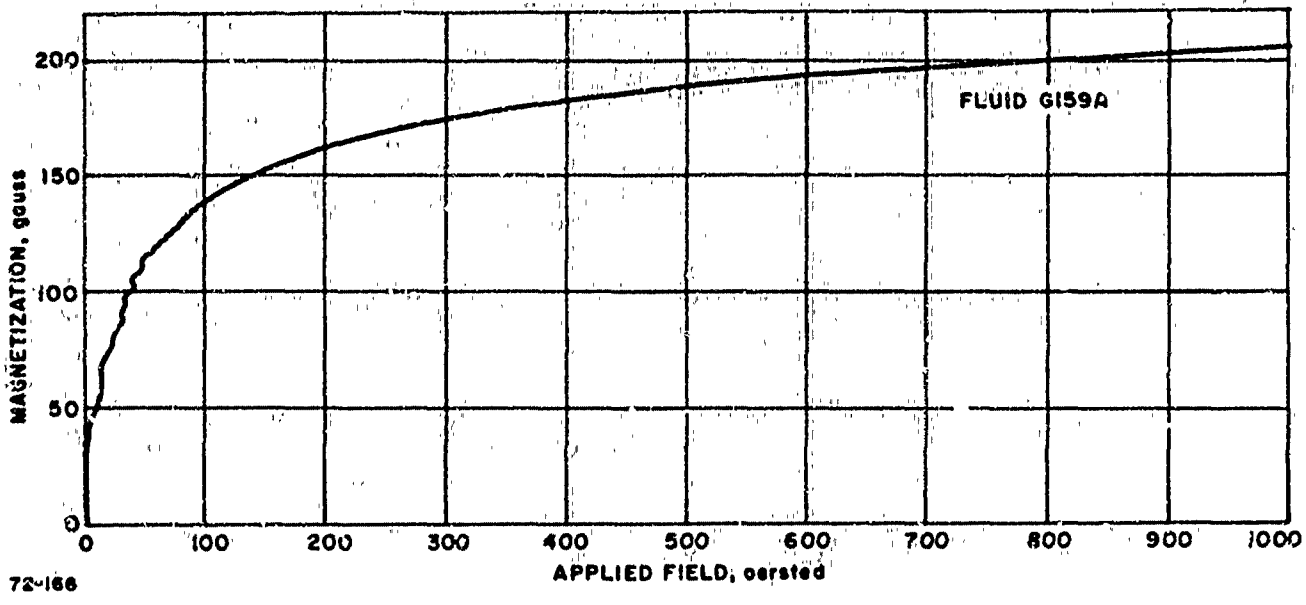

Figure 14 FLUID MAGNETIZATION

frequency below 5 KHz. This implies an effective particle drag radius in excess of 2.00×10^{-6} cm. The presence of a boundary layer of thickness of about 0.70×10^{-6} cm must be postulated to account for this behavior. (This assumed that the original model in which particle to particle interaction was neglected, is still valid.) The presence of such a boundary layer was not in evidence in the d.c. measurements performed earlier.

TABLE III

MAXIMUM FERROFLUID TORQUE

Fluid identification	G159A
Magnetization @ 10,000 oersted, gauss	225
Susceptibility at H = 10 obtained from slope of M vs H curve	2.0
Susceptibility @ H = 10 obtained analytically from measured particle size distribution	1.68
Maximum torque @ H = 10 oersted based χ from M vs H curve	50
Maximum torque @ H = 10 based on χ from particle size distribution	42.2

The present results on the fluid mechanical behavior of the ferrofluid are summarized as follows.

It was seen that fluid torques in the range of up to 100 dyne-cm/cm^3 could be obtained as was predicted from the theoretical studies. The ferrofluid flow pattern was seen to be far more complex than originally postulated. In particular it was noted that the fluid container rotated in a direction opposite to that of the bulk fluid. Thus implying complex, three dimensional flow paths in the bulk of the fluid. This phenomenon was also observed independently in Reference 3. Observations in Reference 2 also pointed to the complex nature of the flow which appeared to be a function of the shape of the container. It was reported in Reference 2 that the fluid rotated coaxially in a cylindrical container; however, in an annular space a number of independent flow cells were established as shown schematically in Figure 15.

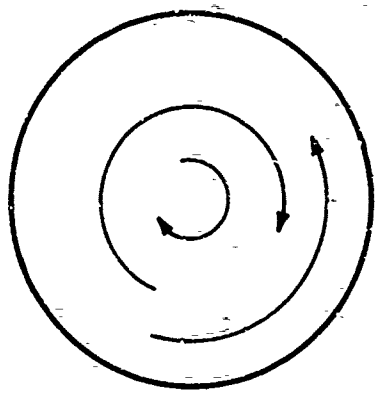

CYLINDRICAL VESSEL

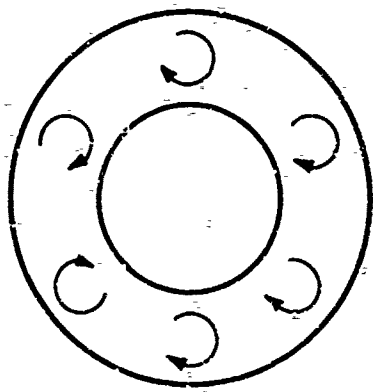

ANNULAR VESSEL

72-167

Figure 15 FLUID FLOW PATTERNS

The preliminary conclusion to be drawn from these observations is that the no radial flow postulate in the earlier studies does not correspond to the observations. This explanation may account for the higher observed rotation rates predicted by the analysis. The particles near free surface of the fluid are subject to different boundary condition than those in the interior or those near the container walls. Presumably in a spherical container, without a free surface, a more regular flow pattern would be obtained.

3. Dynamic Measurements

The purpose of the dynamic measurements is to determine the electronic signal level obtained in a search coil surrounding the rotating mass of ferrofluid as the container is rotated with respect to a reference direction. In this experiment the ferrofluid is enclosed in a sealed vessel surrounded by a search coil. The container assembly is positioned at the intersection of two driving coils. Angular input rates are applied to this entire assembly. The rotating magnetic field causes the individual magnetic particles comprising the ferrofluid to rotate at near synchronous speed. The assembly of angular momenta of these particles may be utilized as a reference in a rate sensor. The precession of the rotating magnetic particles may be detected in a sensitive search coil. The signal from the search coil must be processed to exclude any signal from the driving coils by suitable compensation, or by momentarily switching off the driving field while the search coil signal is analyzed.

a. Experimental Arrangements

For the dynamic experiments the electronics driver circuit was revised to deliver a constant sinusoidal waveform. The block diagram of this system is shown in Figure 16. The two phase generator used in the previous circuit is retained, however, operating at a fixed frequency. A passive non-adjustable filter network is used to yield a sinusoidal waveform. In order to maintain the sinusoidal waveform at the output, a feedback power amplifier is used in each channel.

The details of the circuit are shown in Figure 17. The multivibrators Z1A and Z2B are adjusted to operate at a fixed frequency of 40 KHz. The flip-flops Z2A, Z2B and Z3A are used to divide by four, the "0" and "1" outputs of Z2A give pulses 90° apart to yield the two desired channels. The details of the low pass filter are shown in Figure 17b. A five pole Butterworth filter is used; the circuit elements are identified in the filter schematic. The attenuation of the filter was measured as shown in Figure 18. It is seen that the attenuation is 2 dB at 10 KHz, the desired operating frequency and 16 dB at 15 KHz; this is a satisfactory operating range for the 10 KHz driver.

The feedback amplifier is shown in Figure 17c. A capacitively coupled buffer amplifier connects the signal, via a 2 gang potentiometer (1 gang each used for each channel) to an operational amplifier. The current output of the operational amplifier is connected to the power stage via a Darlington amplifier. The emitter current is fed to the inverting input of the operational amplifier through a resistor network to allow feedback level adjustment. The outputs are connected to the driver coils through series resonance capacitors.

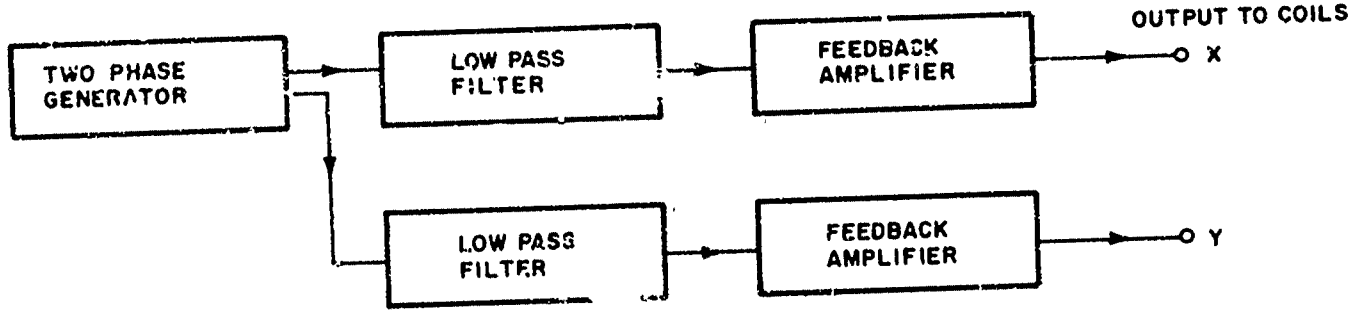

Figure 16 BLOCK DIAGRAM

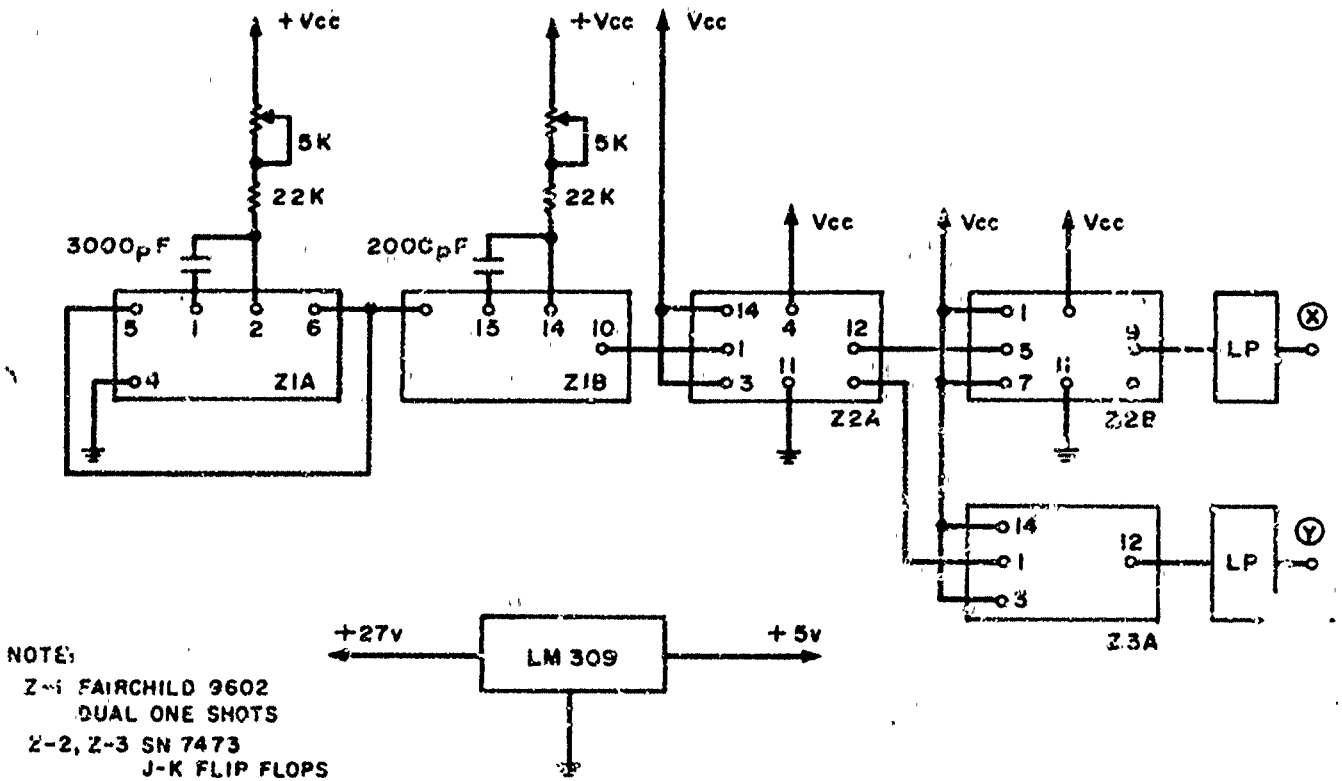

Figure 17a TWO PHASE GENERATOR

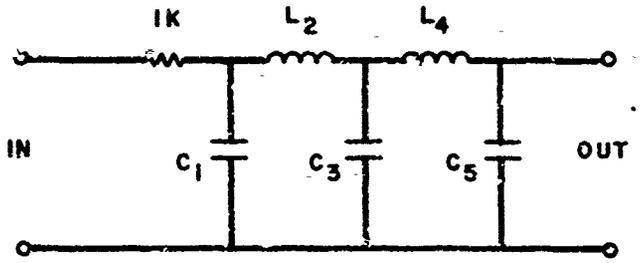

ONE CHANNEL SHOWN
OTHER CHANNEL IDENTICAL

SYMBOL	VALUE	
C_1	4920pF	
L_2	14.22 mH	210 t NO.28 2616 C – A250 389 G
C_2	22,000pF	
L_4	27.0 mH	290 t NO. 28 2616 C – A250 389 W
C	24,600pF	

72-169

Figure 17b LOW PASS FILTER

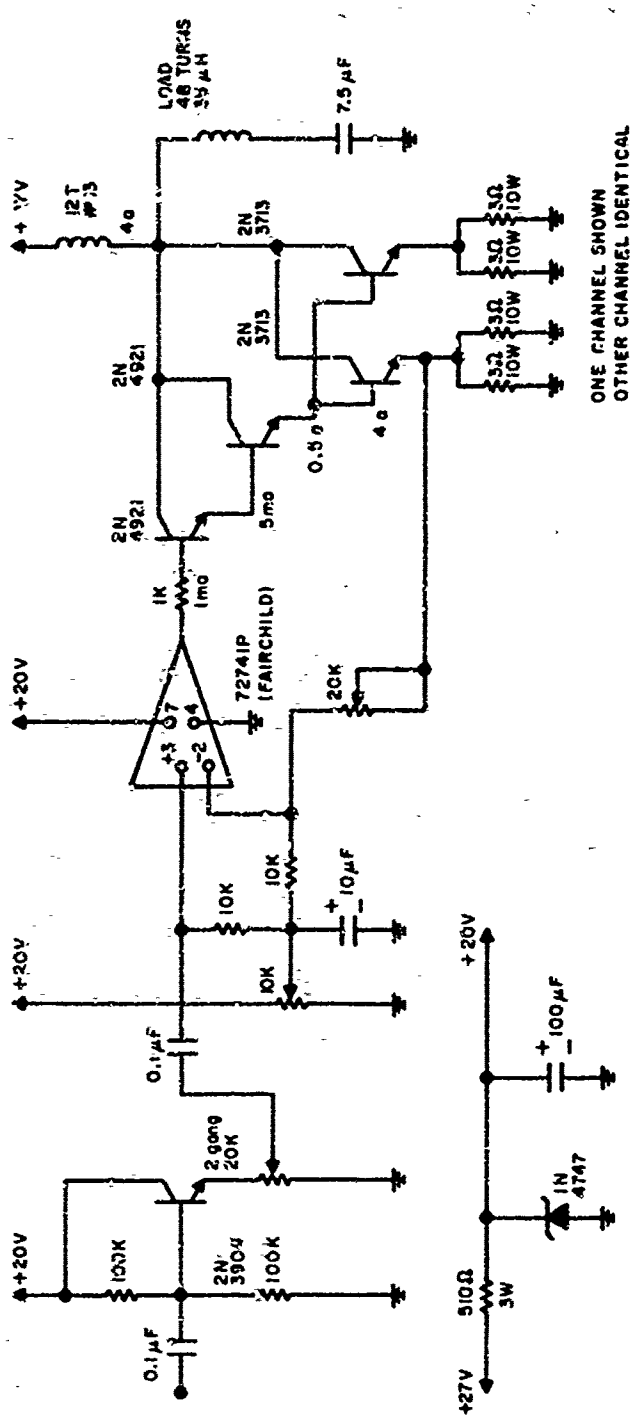

Figure 17c FEEDBACK AMPLIFIER

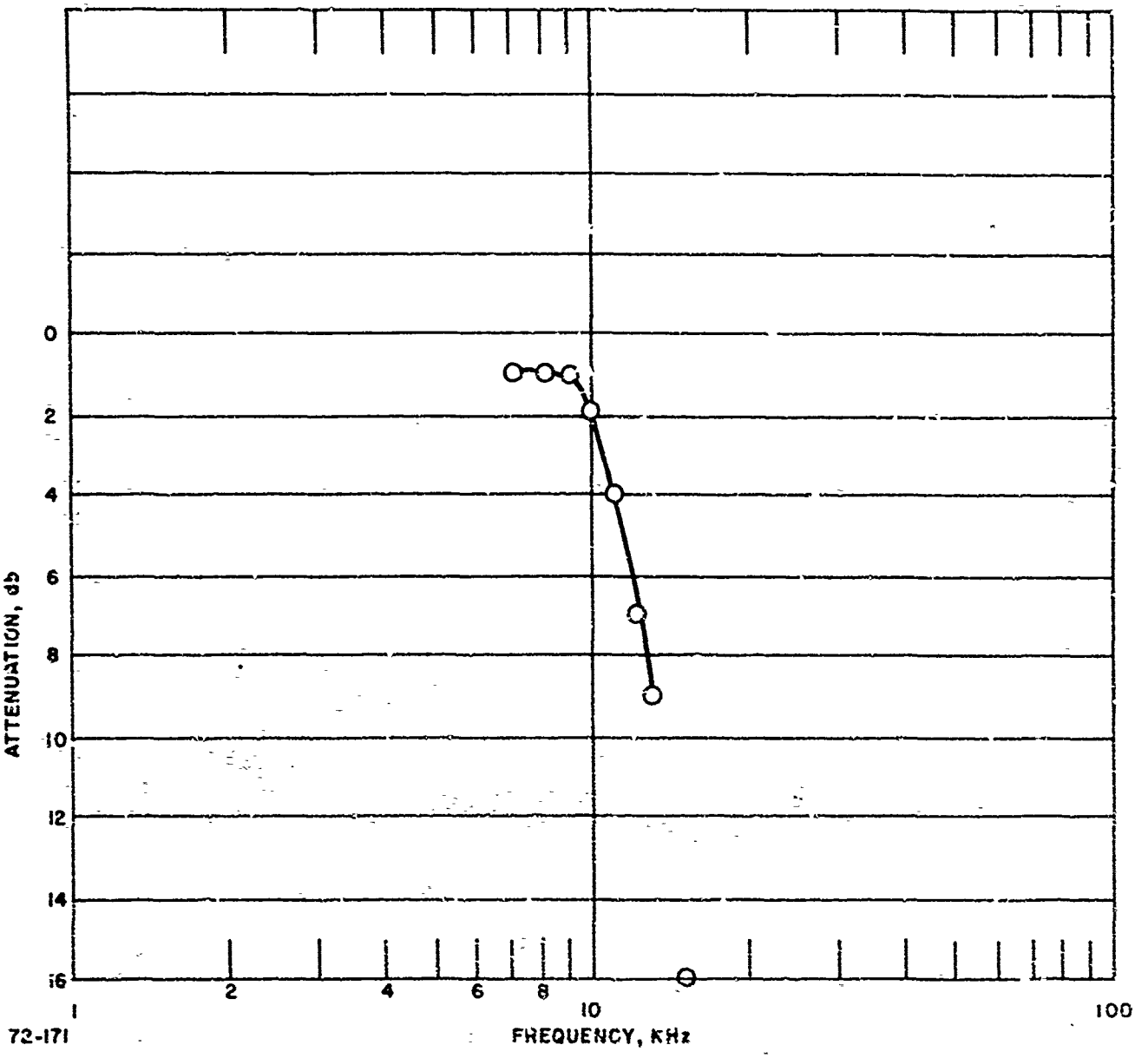

Figure 18 LOW PASS FILTER ATTENUATION

The current delivered to the load was 11 amp pp per channel. Quadrature and sinusoidal waveform were maintained in the coil windings for all current levels, including the maximum value. It is seen from Table I that the magnetic field content for the maximum current was 10.7 oe/amp rms, thus, the maximum value of magnetic field was 83.4 oe.

To study the dynamic effects of the rotating ferrofluid particles a search coil made of 48 turns of #40 wire was wound on a 1.35 cm diameter bobbin. The search coil was placed in the gap and its position was carefully adjusted to minimize the pickup from the driving field. Then the coil was fixed in place with wax. The ferrofluid was placed in a special container designed to exclude entrained air bubbles. The search coil and container are shown in Figure 19.

The entire apparatus was mounted on a base plate, as shown in the photograph of Figure 20. This photograph shows the base plate mounted in the gimbals of a 3 axis table. The orthogonally arranged driver coils are seen on the left of the photograph. The coil form for the search coil is seen at the intersection of the toroidal cores. Immediately below the cores the signal demodulating network is shown. The driver electronics is shown on the left side of the picture. The two phase signal generator is seen near the bottom. The two Butterworth filter are immediately above the signal generator. The operational amplifier is seen immediately above the control knob of the 2 gang potentiometer. The power transistors are mounted on a heat sink, shown near the top of the picture. The series resonant capacitors and current sensing resistors are mounted above the heat sink. A forced air fan, shown at the top completes the assembly. A general view of the experiment is shown in Figure 21. Figure 22 shows the detail of the instrument mounted in the gimbals.

b. Results and Discussion

The dynamic experiment were carried out with a three axis rate table (Carco Electronics). Figure 22 shows a detailed view of the instruments mounted in the inner gimbal of the table. This gimbal has a maximum frequency of 27.5 Hz, a readout accuracy of ±0.12%, a reproducibility of ±0.05%. The maximum angular acceleration rate obtainable is 5,000 degrees/sec^2, the maximum angular velocity 700 deg/sec. The maximum displacement is ±120 deg.

First the electronic assembly was mounted in the inner gimbal of the Carco table without ferrofluid in the gap of the coil. The table was deflected at a rate up to 5 cps with an amplitude of ±15 deg. The output from the search coil, was monitored with a high gain amplifier with a variable band pass. An average position of the table was varied ±90 deg in its plane and ±90 deg in the orthogonal planes. No systematic signals were detected, insuring that there were no spurious signal due to earth gravity or to other fixed permanent magnet sources in the building to interfere with the measurements.

For the dynamic experiments the following signal processing system was used. The driving field was operated at a frequency of 10 KHz, while the assembly was oscillated at up to 5 cps. The position of search coil was adjusted for the minimum pickup from the driving coils by a trial and error procedure. The search coil signal was demodulated by a rectifier and amplified by a band pass amplifier adjusted to bracket the oscillating input rate.

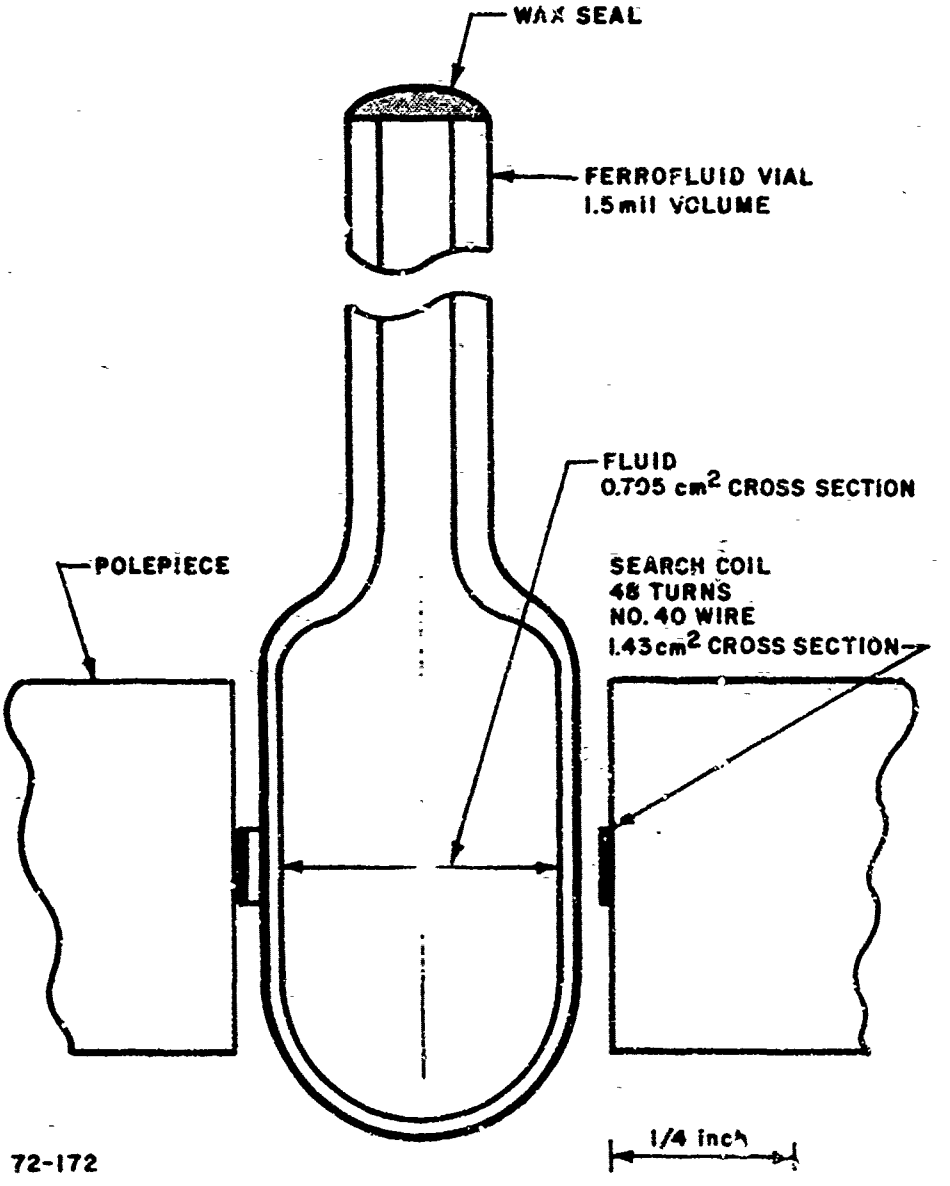

Figure 19 SEARCH COIL AND FERROFLUID CONTAINER

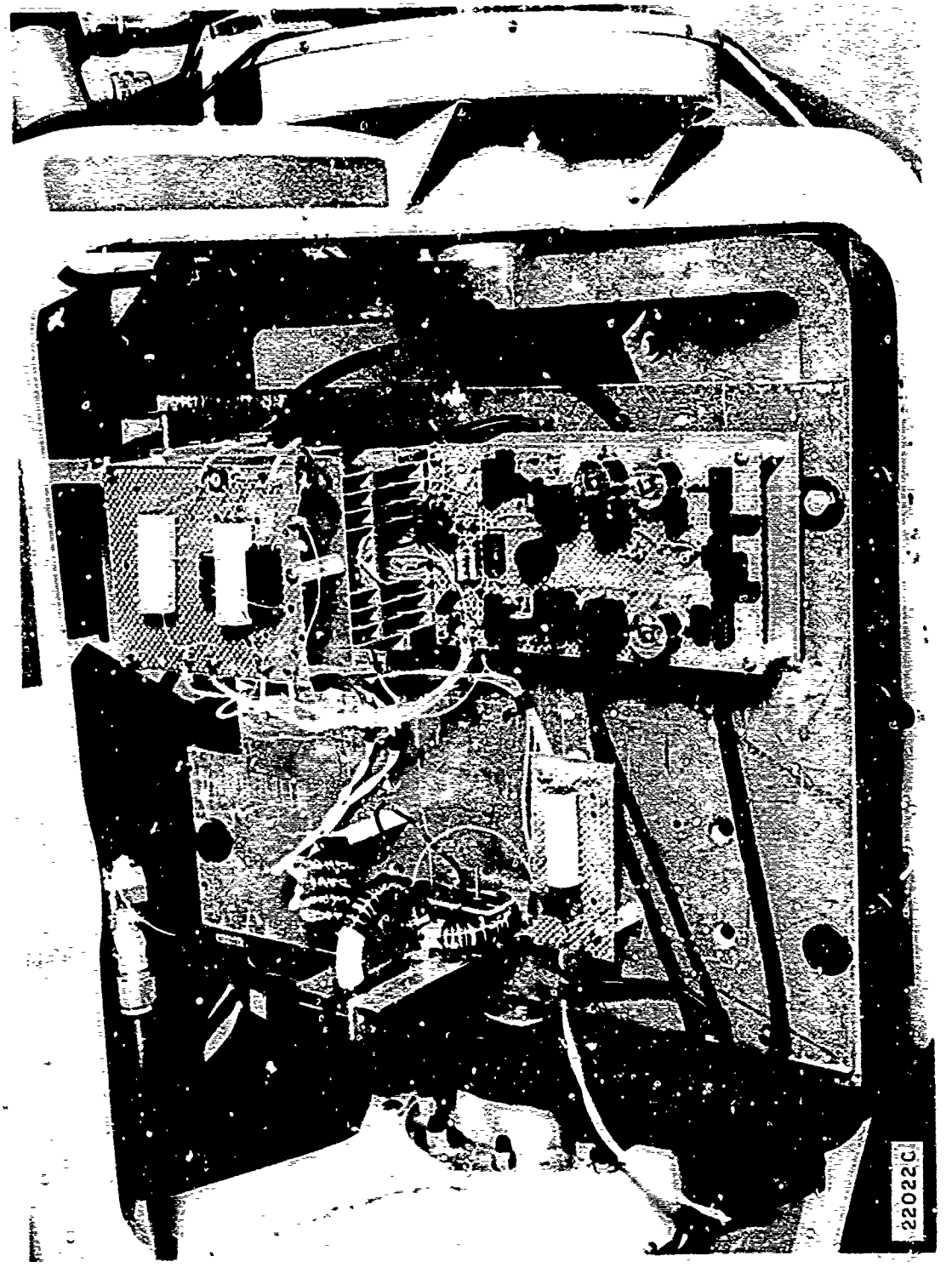

Figure 20 PHOTOGRAPH OF COIL AND DRIVER FOR THE DYNAMIC EXPERIMENTS

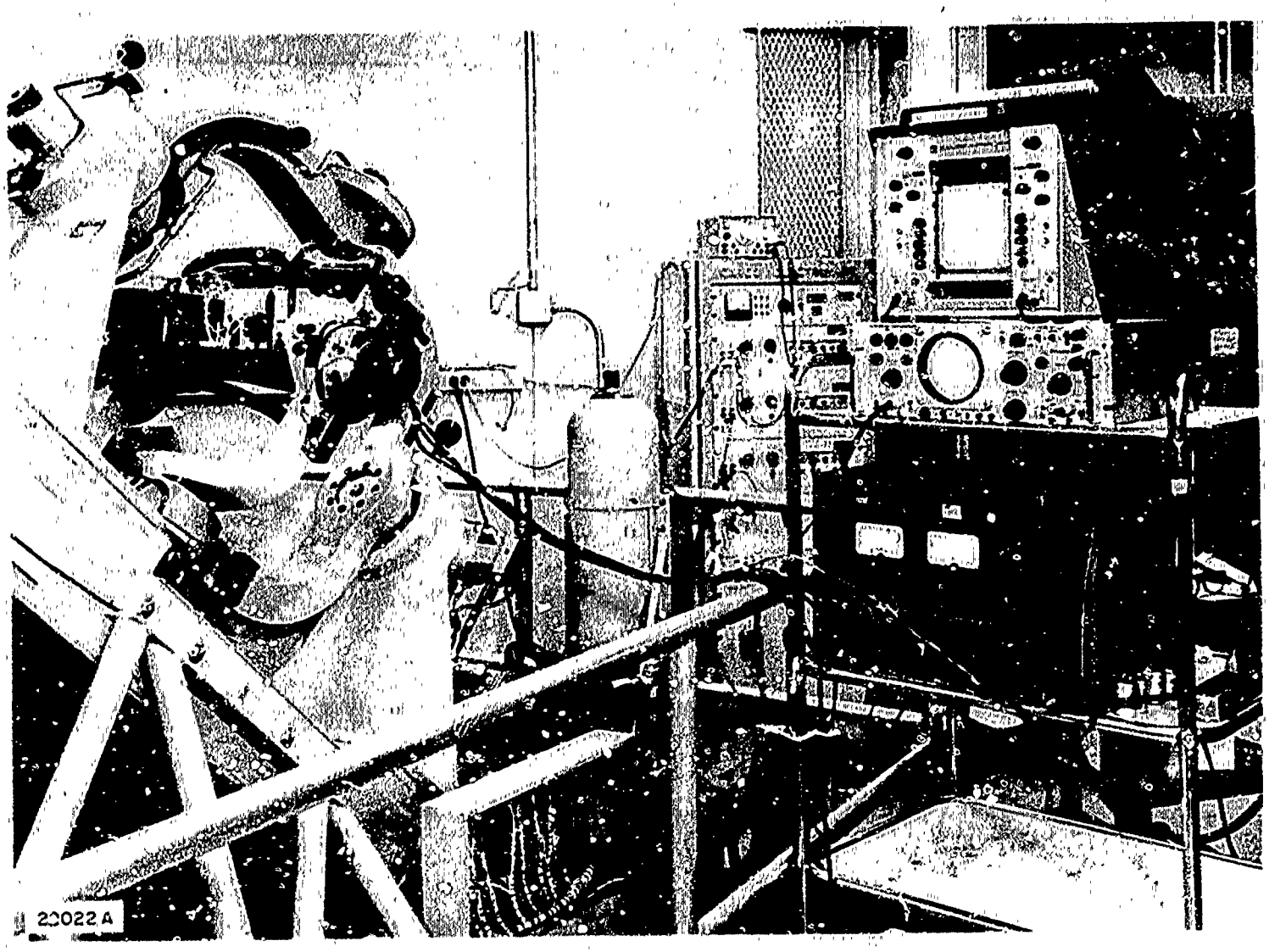

Figure 21 DYNAMIC EXPERIMENTAL SETUP

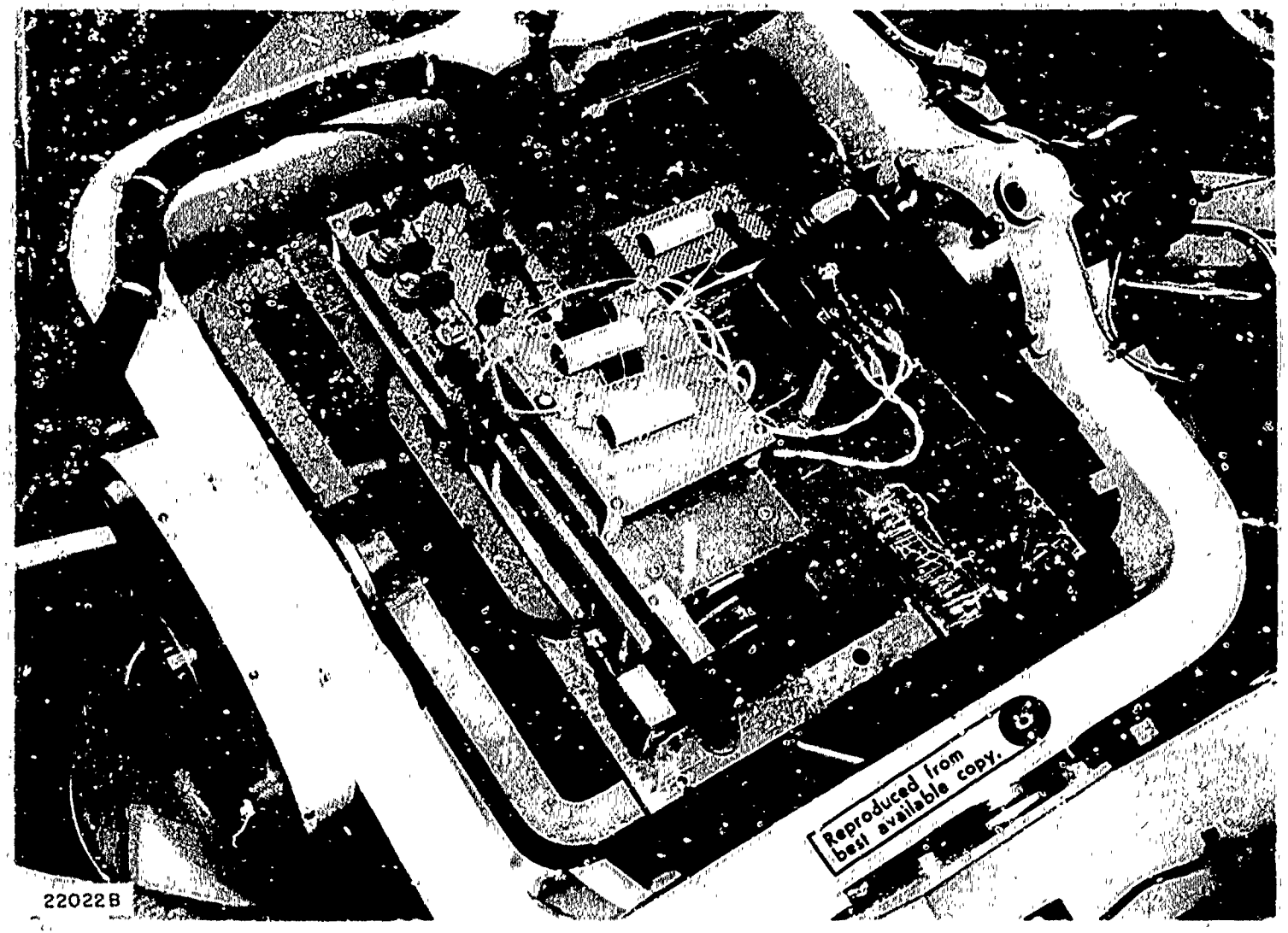

Figure 22 DETAIL OF ELECTRONICS MOUNTED ON RATE TABLE

The dynamic response was observed on a high speed two channel graphic recorder and on an x-y plotter. The results are best illustrated by the x-y plot of Figure 23. The experimental conditions are shown in Table III. It is seen from the study of Figure 23 that noise content of the signal is high, in view of the large signal gain. Because of this, the null signal could not be measured independently. A detailed analysis of the signal proved difficult in view of the high gain employed. The major source of interference on the signal is from frequency components of two phase driver signal not completely filtered out in the pickup and subsequent amplification stage. Further improvement in the signal could be obtained by switching off the driving field for a portion of the cycle and measuring the search coil output when no driving signal is present. In the absence of such an arrangement it is assumed that the gyro signal is at most equal to the total signal level observed, as shown in Table IV. Thus, the instrument scale factor may be calculated to be 0.274 μvolt/milliradian.

TABLE IV

DYNAMIC EXPERIMENTS

Ferrofluid Code	G159A
Coil Excitation, amp p-p per channel	11
Search Coil: Number of turns	48
Cross sectional area, cm^2	1.43
Operating Frequency, KHz	10
Total resultant magnetic field, oersted	88
Table Rate, Hz	5
Table Deflection, deg p-p	31.8
Total signal observed, μ volts, p-p	0.148
Instrument scale factor, μ volts/radian	0.274

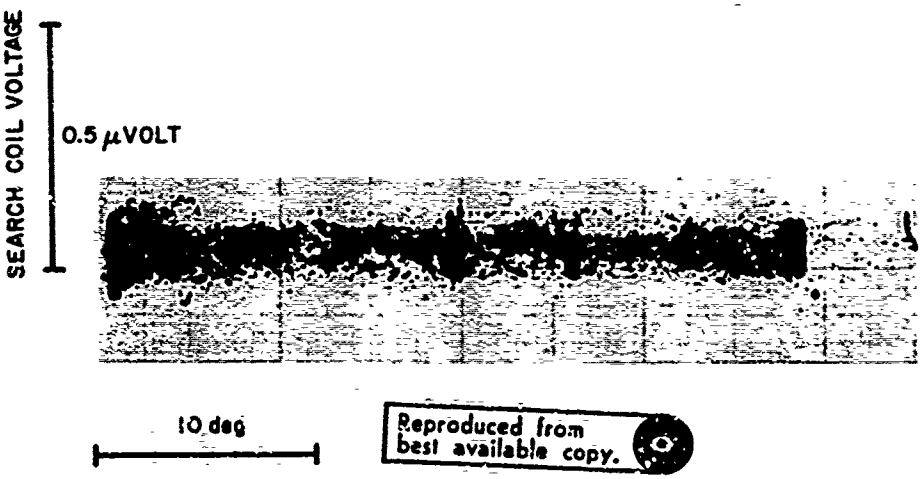

Figure 23 DYNAMIC RESULTS

SECTION III

CONCLUSIONS

In this study a rotating electromagnetic field is coupled to a nonconducting magnetic liquid, a ferrofluid, and liquid torque and rotation are observed. The experimental results of torque reported here are in accordance with the general trends previously predicted. Experimental fluid torques of up to 100 dyne-cm/cm^3 were transmitted by a driving field of 80 oersteds rotating at rate of 5 KHz. The maximum torque transmission occurred at a frequency lower than predicted by prior theory, which took into account the disorienting effects of Brownian Motion and the experimentally observed particle size distribution. To apply the theory to the results of this study the thickness the boundary layer surrounding each particle must be taken into account in calculating the effective partic. radius. The boundary layer thickness is equal to the radius of the particle.

The presence of complex fluid motions in the interior of the ferrofluid were evidenced in an experiment where the surface of the ferrofluid rotated in a direction opposite to that of the bulk fluid.

In a dynamic experiment a volume of ferrofluid driven by an 80 oersted field at 10 KHz and surrounded by an electromagnetic pickup coil was subjected to angular rates of up to 150 degrees/sec. The demodulated search coil signal was seen to be no greater than 0.2 μ volts/milliradian.

It was seen that, the electromagnetically induced ferrofluid torque is significant, that the flow is far more complex than originally postulated, and that useful rate signals could not be obtained using convectional signal processing techniques.

REFERENCES

1. Moskowitz, R., and Rosensweig, R.E., "Nonmechanical Torque-Driven Flow of a Ferromagnetic Fluid by an Electromagnetic Field", Applied Physics Letters 11 (10), 301-303 (1967)

2. Rosen weig, R.E., "Torque and Fluid Motion in Response to a Rotating Magnetic Field in Ferrofluids Composed of Colloidal Particles Subject to Thermal Agitation", Avco Technical Release (October 1967).

3. Miskolczy, G., Litte, R., and Kaiser, R., Ferrofluid Particle Gyro, AFFDL-TR-70-5, February 1970.

4. Brown, R.C., University of Sheffield, England, as referenced by Rosensweig, R.E., "Progress in Ferrohydrodynamics", Industrial Research, October 1970.

5. Timoshenko, S., Strength of Materials, Part 1, p. 290, New York, 1956.

6. Brandrup, J., Immergut, E.H., Polymer Handbook, p. IV-82, John Wiley & Sons, 1966.